AD-A063 539 SCIENCE APPLICATIONS INC MCLEAN VA F/G 18/3
INVESTIGATION OF LARGE SCALE OPTICAL FLASH SOURCES.(U)
APR 78 J E COCKAYNE, T M KNASEL DNA001-77-C-0231
UNCLASSIFIED SAI-78-694-WA DNA-4617F NL

1 OF 1
AD
AD63539

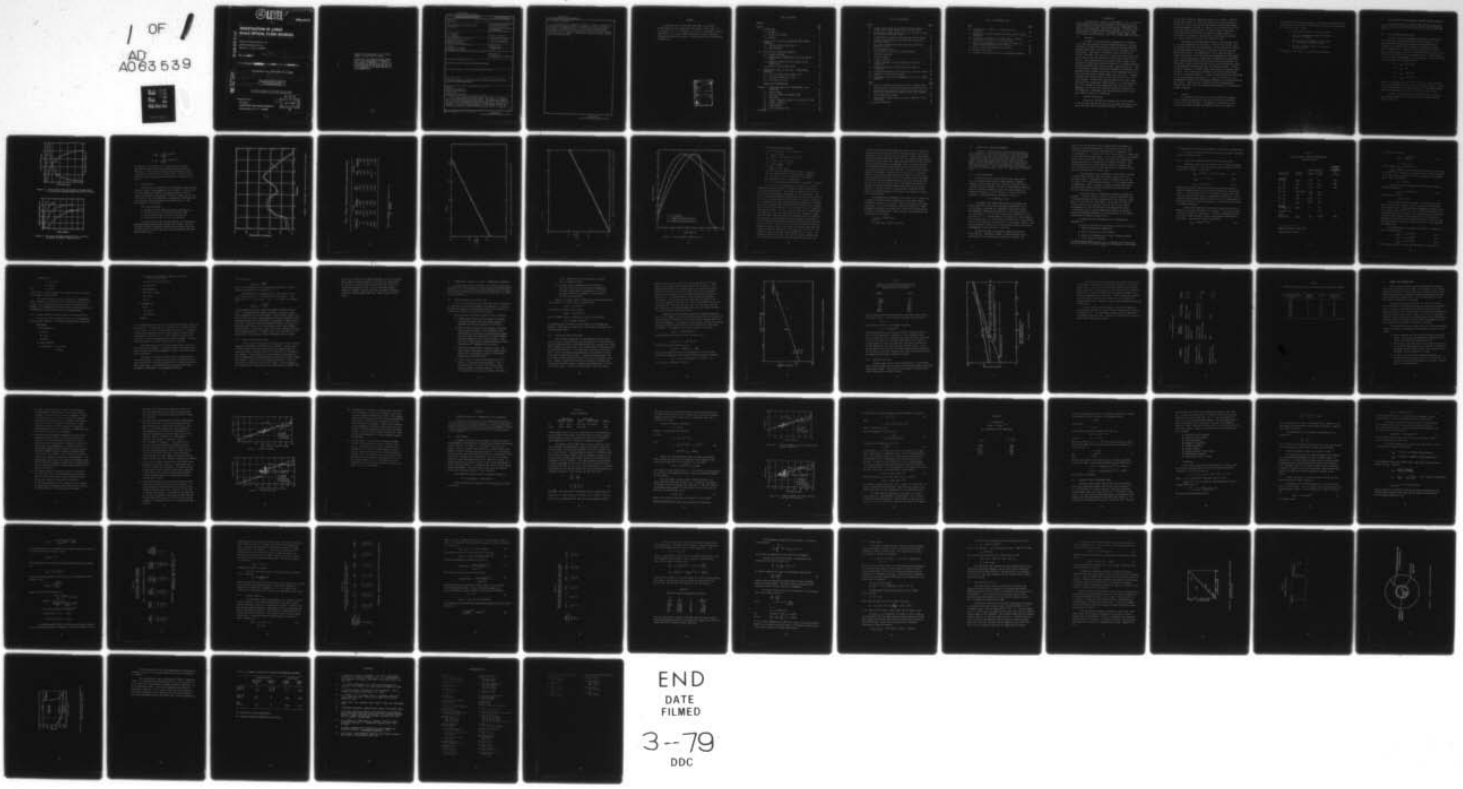

END
DATE
FILMED
3-79
DDC

(12) LEVEL III

(15) DNA 4617F

SBIE

5C

(6)

INVESTIGATION OF LARGE SCALE OPTICAL FLASH SOURCES

Science Applications, Inc.
8400 Westpark Drive
McLean, Virginia 22101

(11) 30 April 1978

(12) 73 p.

(14) SAI-78-694-WA

(9) Final Report, 6 June 1977—31 January 1978

(10) CONTRACT No. DNA 001-77-C-0231

J. E. Cockayne,
T. M. Knasel
M. D. McDonnell

(15)

(16) 125AAXY (17) X96P

THIS WORK SPONSORED BY THE DEFENSE NUCLEAR AGENCY
UNDER RDT&E RMSS CODE B322077462 I25AAXYX96008 H2590D.

62710H

Prepared for
Director
DEFENSE NUCLEAR AGENCY
Washington, D. C. 20305

408 484

78 11 21 027

Destroy this report when it is no longer needed. Do not return to sender.

PLEASE NOTIFY THE DEFENSE NUCLEAR AGENCY, ATTN: TISI, WASHINGTON, D.C. 20305, IF YOUR ADDRESS IS INCORRECT, IF YOU WISH TO BE DELETED FROM THE DISTRIBUTION LIST, OR IF THE ADDRESSEE IS NO LONGER EMPLOYED BY YOUR ORGANIZATION.

UNCLASSIFIED

SECURITY CLASSIFICATION OF THIS PAGE *(When Data Entered)*

REPORT DOCUMENTATION PAGE		READ INSTRUCTIONS BEFORE COMPLETING FORM
1. REPORT NUMBER DNA 4617F	2. GOVT ACCESSION NO.	3. RECIPIENT'S CATALOG NUMBER
4. TITLE *(and Subtitle)* INVESTIGATION OF LARGE SCALE OPTICAL FLASH SOURCES		5. TYPE OF REPORT & PERIOD COVERED Final Report for Period 6 Jun 77—31 Jan 78
		6. PERFORMING ORG. REPORT NUMBER SAI-78-694-WA
7. AUTHOR(S) J. E. Cockayne T. M. Knasel M. D. McDonnell		8. CONTRACT OR GRANT NUMBER(S) DNA 001-77-C-0231
9. PERFORMING ORGANIZATION NAME AND ADDRESS Science Applications, Inc. 8400 Westpark Drive McLean, Virginia 22101		10. PROGRAM ELEMENT, PROJECT, TASK AREA & WORK UNIT NUMBERS Subtask I25AAXYX960-08
11. CONTROLLING OFFICE NAME AND ADDRESS Director Defense Nuclear Agency Washington, D.C. 20305		12. REPORT DATE 30 April 1978 13. NUMBER OF PAGES 72
14. MONITORING AGENCY NAME & ADDRESS*(if different from Controlling Office)*		15. SECURITY CLASS *(of this report)* UNCLASSIFIED 15a. DECLASSIFICATION/DOWNGRADING SCHEDULE

16. DISTRIBUTION STATEMENT *(of this Report)*

Approved for public release; distribution unlimited.

17. DISTRIBUTION STATEMENT *(of the abstract entered in Block 20, if different from Report)*

18. SUPPLEMENTARY NOTES

This work sponsored by the Defense Nuclear Agency under RDT&E RMSS Code B322077462 I25AAXYX96008 H2590D.

19. KEY WORDS *(Continue on reverse side if necessary and identify by block number)*

Modeling
Nuclear Burst Detection
Nuclear Flash Simulation
Thermal Pulse
Thermochemical Reactions

20. ABSTRACT *(Continue on reverse side if necessary and identify by block number)*

This report analyzes the use of optical flash sources in testing of Nuclear Burst Detection System (NBDS) devices. The primary case studied is that of the use of thermochemical reactions to simulate nuclear fireballs. The report reviews the NBDS requirements and weapon output, contrasting the outputs of a variety of simulation sources. Of the sources studied, the thermochemical reactions require detailed modeling, and this is reported.

(over)

DD FORM 1 JAN 73 1473 EDITION OF 1 NOV 65 IS OBSOLETE

UNCLASSIFIED

SECURITY CLASSIFICATION OF THIS PAGE *(When Data Entered)*

20. ABSTRACT (Continued)

Two general types of models are reported. The first is based on very simple thermal behavior but predicts the growth of fireballs in agreement with previous thermochemical tests of a wide variety of types and sizes. The second type of model considers each step in detail in the fireball development. This is useful for tailoring of the fireball output. Detailed data comparison with a number of thermochemical reaction tests and recommendations conclude the report.

PREFACE

The authors wish to thank Major James Mayo of the Defense Nuclear Agency for assistance during the conduct of this study. Mr. J. Dishon, III, Mr. B. S. Chambers, III, and Dr. W. Koechner of Science Applications, Inc., and Mr. Dean Thornborough of Sandia Laboratory, Albuquerque, New Mexico assisted in providing data for the calculations reported here.

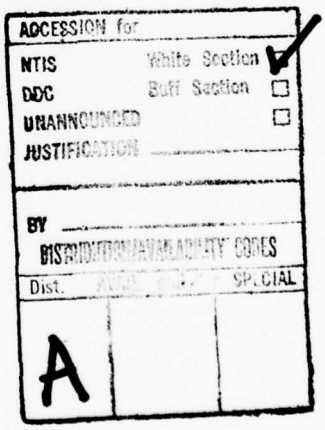

TABLE OF CONTENTS

LIST OF ILLUSTRATIONS

LIST OF ILLUSTRATIONS (cont.)

I INTRODUCTION

The Nuclear Burst Detection System (NBDS) relies on processing optical pulses from above ground nuclear weapon detonations to provide information to battlefield commanders. The system performance needs to be verified under realistic conditions of atmospheric transparency, cloud reflections, and terrain shadowing. A recently developed concept for a thermochemical flash generator appears to offer promise for a fieldable source. The primary purpose of this report is to evaluate the potential for a low cost, reliable NBDS test system.

I.1 Rationale

In order to equip battlefield commanders with information on the times and locations of nuclear weapon detonations in wartime situations, a Nuclear Burst Detection System has been developed that relies on (among other signals) the optical pulse signature of an air burst weapon. This report is concerned solely with the optical portion of the NBDS, and the desire to provide an optical source that will trigger and test the system over a wide range of realistic conditions. Such considerations as the optical pulse risetime, width and intensity observed by the optical detectors in an NBDS are primarily functions of weapon yield, height of burst, range and direction. They will be modified, perhaps seriously, by atmospheric transparency, cloud shadowing and/or secondary reflections, terrain shadowing and reflections, and the effects of weather (haze, rain, fog, etc.). Lightning discharges (particularly the rare super-lightning type) may provide false triggers. A system test with simulated nuclear pulses would resolve areas of uncertainty in NBDS response. It is the purpose of this work (drawing on recent experimental data on optical flash generators) to calculate the theoretical conditions required for a valid NBDS test. Furthermore, test system configurations of likely use in NBDS validation are recommended.

I.2 Optical Flash Sources

A source for the NBDS tests requires very high brightness in the pass band (visible and near IR), reasonably wide angular divergence, and controllable risetime and duration. These conditions

may rule out a number of conventional choices (e.g. lasers). Recently Science Applications, Inc. (SAI) has completed an initial development program for a large scale optical flash generator based on high temperature thermochemical reactions.[1,2] Tests of a field proven low cost unit of 10^9 watts peak power and above 10^8 joules of optical energy have raised the possibility of use of this device for NBDS validation. In this report an assessment of the potential of themochemical reactions as a source of optical test pulses for the NBDS is made.

Development of the thermochemical optical flash generator prior to this work concentrated on the aspects of one specific reaction, that of aluminum oxidation at high temperatures. Initial theoretical research had isolated metallic oxidization as a potential source of large scale optical flash output. The temperature of such a radiating system is limited on the upper side by the vaporization temperature of the metallic oxide. Alumina (Al_2O_3) with a vaporization temperature of around 3800^oK (see Appendix) would allow radiation fluxes of about 200 cal/cm^2sec if a sufficiently optically thick cloud of Al and O_2 can be created and ignited at high temperature forming Al_2O_3 near the vaporization point. Aluminum is readily available in various finely divided forms, is inexpensive and is non-toxic. Thus, previous work proceeded to ascertain the experimental details of a practical generator. A series of about 50 tests were performed in 1976 and reported by Cockayne et al.[1] Later a series of over 100 thermochemical reaction test firings were conducted in a continuing development series[2]. These and open literature sources on thermochemical reaction tests form a basis for theoretical development of the application to NBDS validation.

I.3 Approach

The usefulness of any optical source for NBDS testing depends on the trigger requirements set by the sensor system and on the objectives set for system validation. The approach in this report will be to review and relate the NBDS requirements for the optical output of

both nuclear and thermochemical devices. To do this, development of the expected output of large scale thermochemical reactions will be inferred as scaling laws based on data.

In summary the key issues to resolve are these:

1) Does the thermochemical generator provide a trigger for the NBDS?

2) What are the basic equations that describe the thermochemical generator output?

3) Are there alternate schemes of calibration that hold promise?

The purpose of this report is to answer these questions.

II OPTICAL OUTPUT OF NUCLEAR WEAPONS AND NBDS RESPONSE PARAMETERS

The optical output of airburst nuclear weapons will be parametrized versus yield, range and height of burst. These predictions will be contrasted with the expected trigger requirements of the NBDS system.

II.1 Nuclear Weapon Optical Output

The first task of the reported work requires a characterization of the optical (thermal) waveforms of nuclear bursts. It is well known that airburst nuclear weapons have a unique optical signature consisting of a first rapid pulse followed by a slower and much longer pulse. The time of the peak of the first pulse is t_{1max}, similarly t_{2max} is the time of the second peak, and t_{min} is the time from initiation to the minimum between pulses. The most general review of nuclear phenomonology - that of Glasstone - quotes the following relationships for the thermal output:[3]

$$\text{II.A.} \quad P_{max} = 4W^{\frac{1}{2}} \text{ cal/sec}$$

$$\text{II.B.} \quad E_{tot} = W/3$$

$$\text{II.C.} \quad t_{min} = 2.5W^{\frac{1}{2}} \text{ msec}$$

$$\text{II.D.} \quad t_{2max} = 32W^{\frac{1}{2}} \text{ msec}$$

where W is the weapon yield in KT (1KT = 10^{12} cal). The first pulse contains approximately 1 percent of the total thermal output. Figure 1 is taken from Reference 3 and contains details of the normalized pulse shape (second maximum only) and total output for various yields.

In order to calculate flux ($\dot{Q}$) and fluence (Q) at a distant point, ground range R from a burst of H height, we need additional formulas; they are:

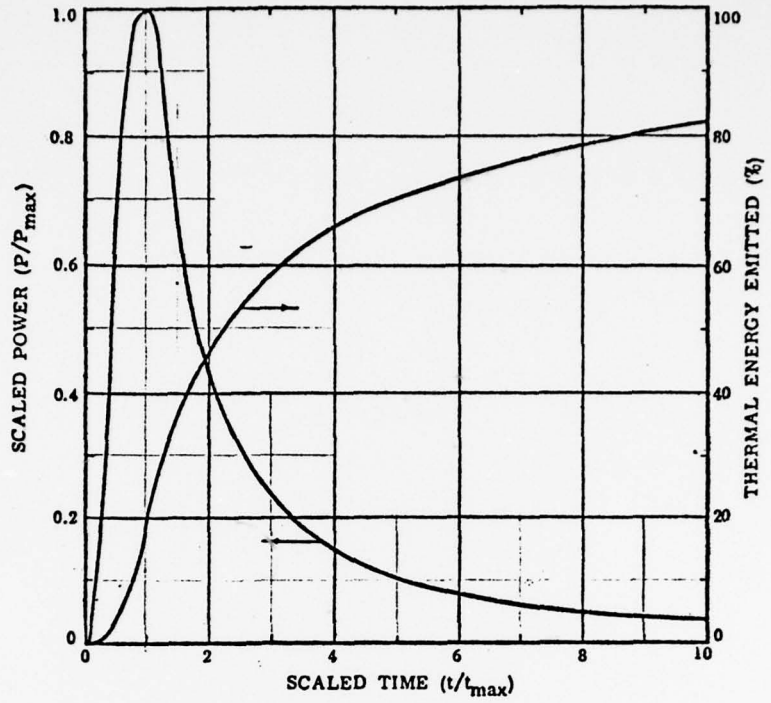

Figure 1a. Scaled Fireball Power and Fraction of Thermal Energy vs. Scaled Time in Second Thermal Pulse of an Air Burst.

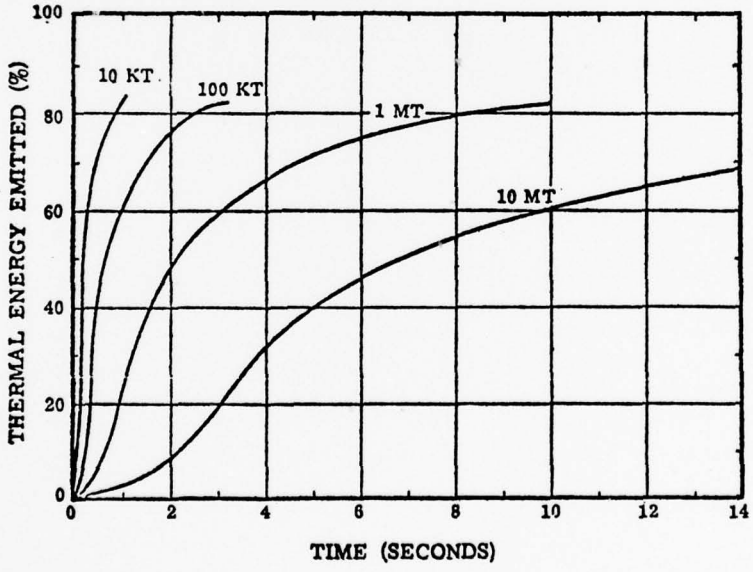

Figure 1b. Percentage of Thermal Energy Emitted as a Function of Time for Air Bursts of Various Yields.

$$Q = \frac{W}{12\pi} \quad \frac{10^8}{(H^2+R^2)} \ (Cal/cm^2)$$

$$\dot{Q} = \frac{W}{\pi} \quad \frac{10^8}{(H^2+R^2)} \ (Cal/cm^2 \ sec)$$

No atmospheric transmission loss is included in these formulae. Additional estimates of the time spectrum have been obtained from Reference 4. Figure 2 shows an example of one of these and, Table 1, a compilation of pertinent data at several yields. Figures 3 and 4 summarize the t_{min} and t_{2max} calculation (Table 1) and formula of Reference 3.

II.2 NBDS Operation

Optical pulses are detected by a Si based detector whose response function is shown in the accompanying figure (Figure 5). There are four real time hardware discriminants that determine whether an event is likely to be a nuclear event and which, therefore, trigger the retention of 0.32 msec of data in the NBDS memory, accumulation of additional data, and activation of the microprocessor discriminant analysis. These discriminants are listed below.

Real Time Discriminants

1) VHF Negative Pulse exceeding a specific threshold 5 v/m
2) VHF Arrival within 1 millisecond of optical trigger
3) Optical signal trigger level $>6.3 \times 10^{-7}$ watts/cm^2
4) Optical rate of rise $>2.1 \times 10^{-3}$ watts/cm^2/sec

The first two of the real time discriminants are electromagnetic pulse discriminants which are not relevant to our problem. The last two merely indicate a significant increase above an ambient light threshold and a rate of rise consistent with, but not exclusively associated with, a nuclear event.

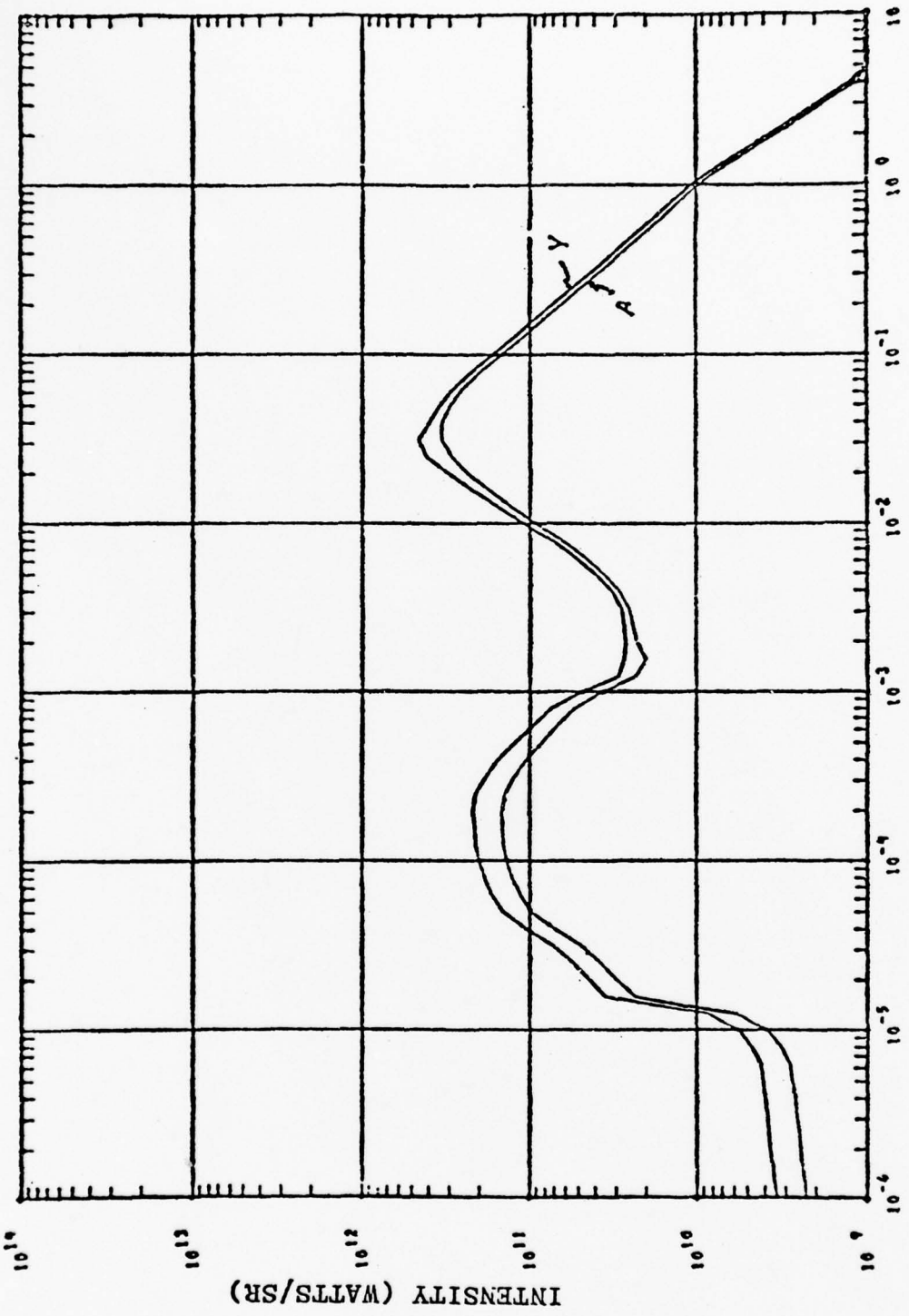

Figure 2. In-Band Power at Source for Two Broad Band Silicon Sensors

Table 1. Results of Detailed Calculations of Nuclear Thermal Output

Yield (KT)	1st Max Time	1st Max Intensity	Min Time	2nd Max Time	2nd Max Intensity
0.1	10^{-4}	$5\ 10^{10}$	$6\ 10^{-4}$	10^{-2}	10^{11}
1.0	2.10^{-4}	$1.7\ 10^{11}$	$2\ 10^{-3}$	$3\ 10^{-2}$	$4\ 10^{11}$
10.0	2.10^{-4}	$7\ 10^{11}$	$9\ 10^{-3}$	10^{-1}	$1.5\ 10^{12}$
100.0	10^{-3}	$2\ 10^{12}$	$2\ 10^{-2}$	$2.5\ 10^{-1}$	$7\ 10^{12}$
1000.0	10^{-3}	$7\ 10^{12}$	$6\ 10^{-2}$	.9	$2\ 10^{13}$

Units: Intensity - Watts per steradian at 1 km
Time - Seconds

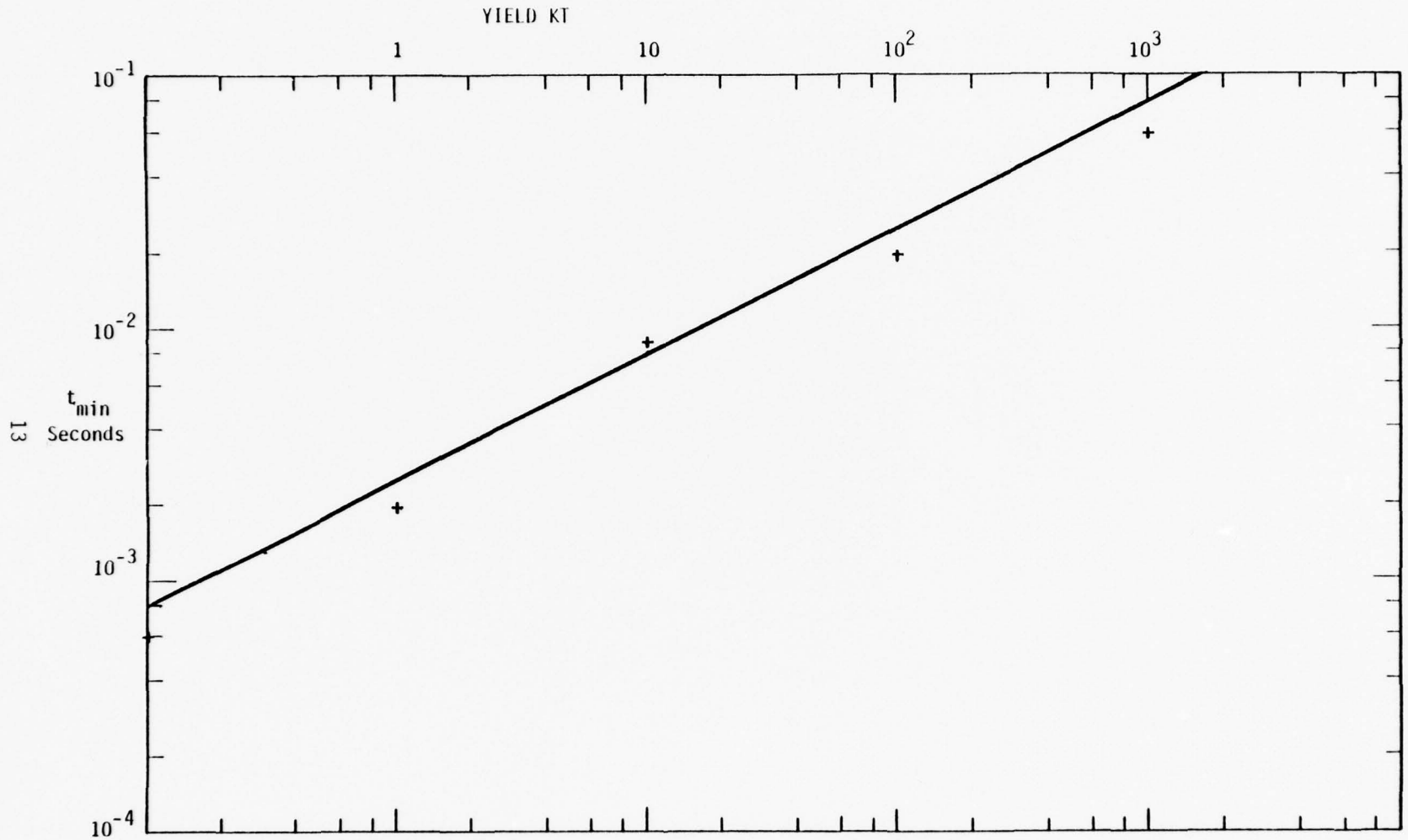

Figure 3. t_{min} curve from Glasstone versus Detailed Calculations at Various Yields

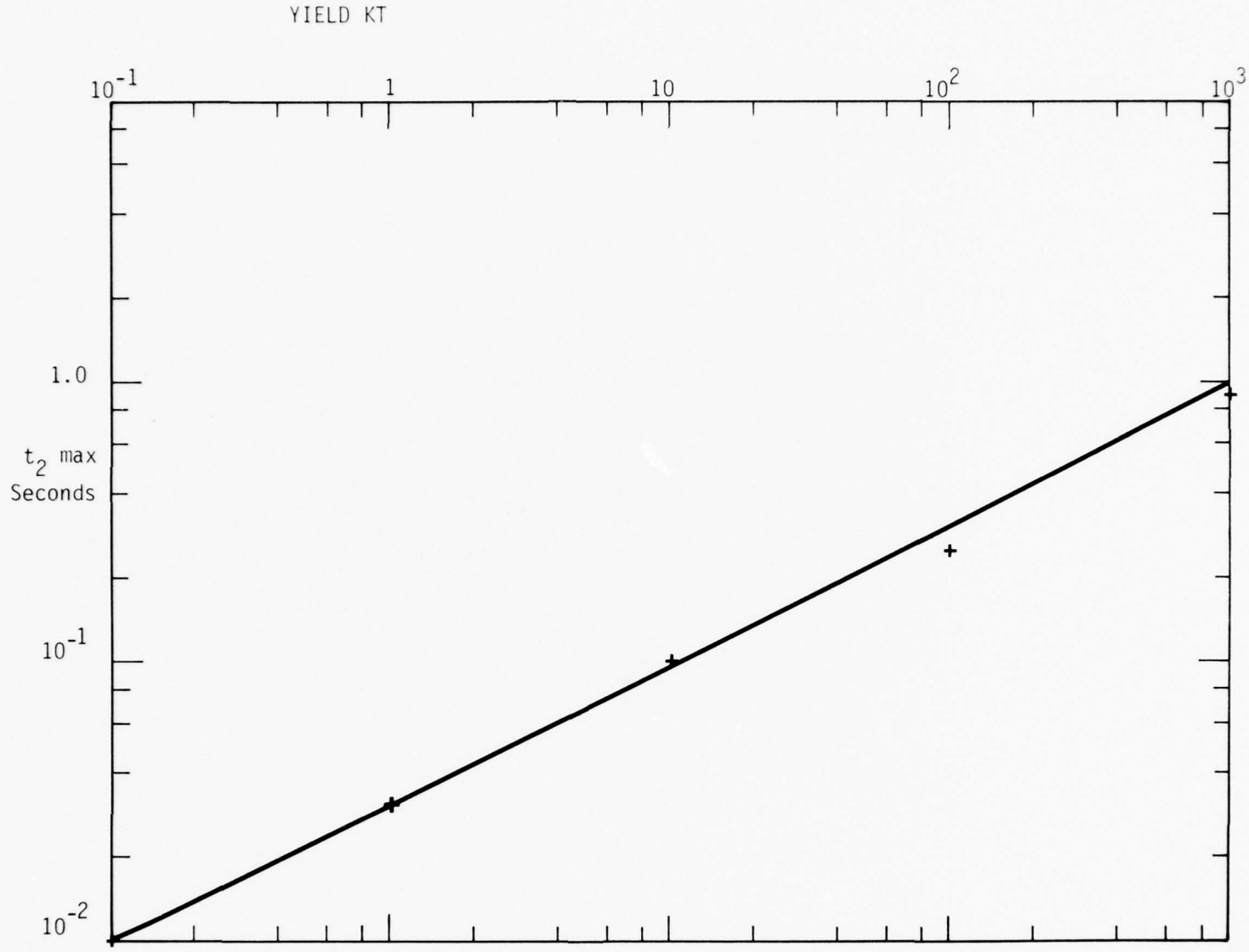

Fig. 4 $t_2$max curve from Glasstone versus Detailed Calculations at Various Yields

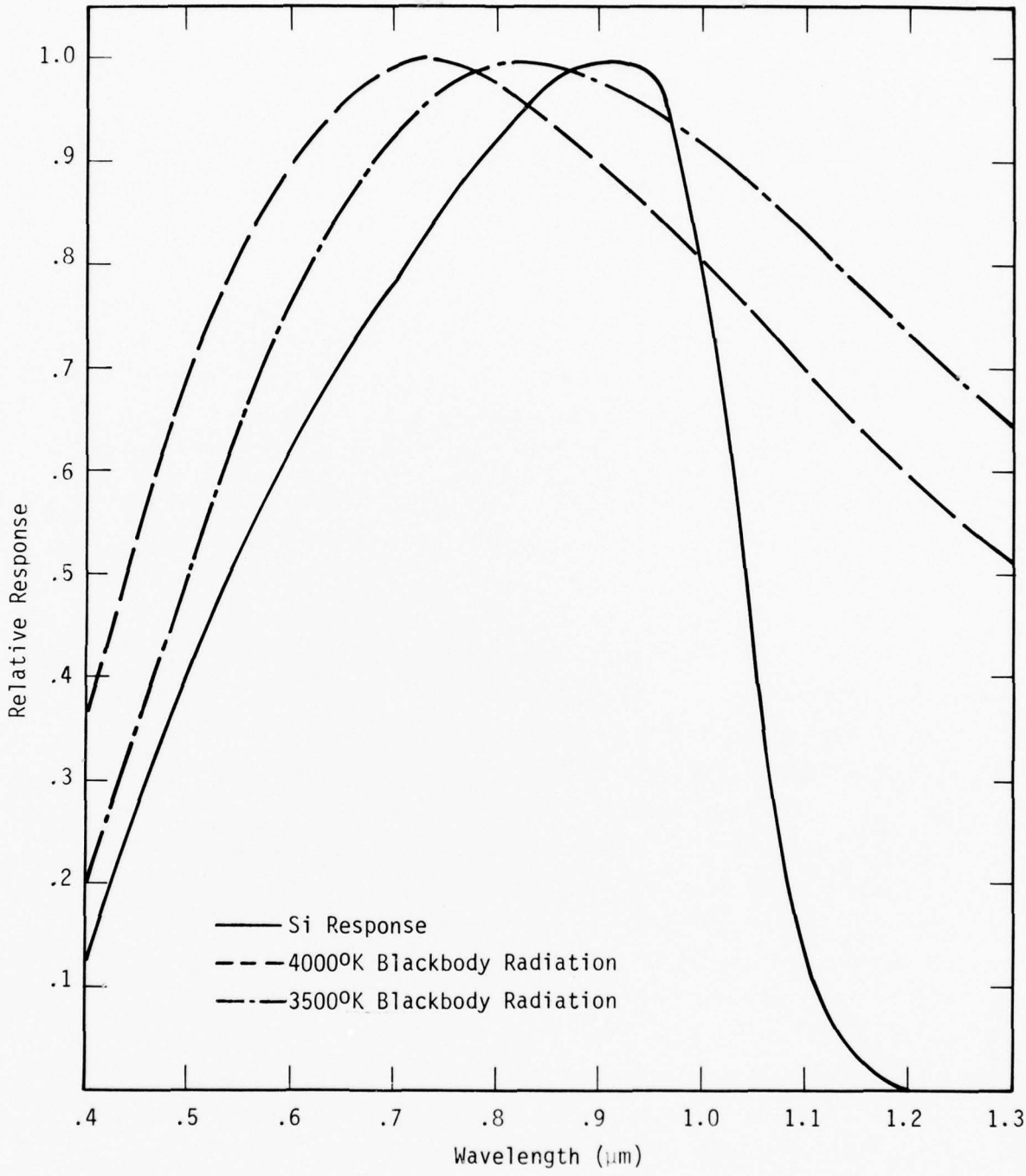

Figure 5. Silicon Detector Response Curve

Microprocessor Discriminants

1) First sample $>6.3 \times 10^{-7}$ watts/cm^2
2) $t_{1max} < 3.6$ msec
3) time of (first max/6.25)> 0.5 msec
4) $5\ t_{1max} < t_{min} < 70\ t_{1max}$
5) $4\ t_{min} < t_{2max} < 20\ t_{min}$
6) $t_{min} < 199$ msec
7) Width of min $< 8\ t_{min}$
8) 88 of the 264 samples before 100 msec $> t_{1max}/6.25$
9) Flat long duration first peak pulses are rejected
10) First max > avg. amplitude of up to 128 samples
11) Second max > 6.25 : min amplitude
12) First ten samples after second max > second max : (6.25/3)

The first of the microprocessor discriminants is presently redundant but could be varied to exclude low yield, distant bursts from further consideration. The second is a check on the rise time of the first maximum which is applicable to all normal yields. The third is actually performed by checking that the amplitude of the pulse at 0.5 msec is greater than 1/6.25 of the first maximum. (The factor 6.25 is equivalent to the difference between any consecutive 32 analog to digital conversion steps in the sensitivity range of the instrument and is used by the microprocessor as a consistent figure for measuring amplitude variations.) If this is the case then the first maximum has not formed by 0.5 msec and consequently the first maximum is broader than this value. The fourth and fifth determine the arrival times of the minimum and second maximum in terms, ultimately, of the width of the first maximum and are consistent with all yields within the range of 0.1 KT to 1 MT. The sixth is satisfied by all normal yields and is an absolute check on the arrival time of the minimum rather than one related to the first peak arrival time (t_{1max}) as in the fourth. The seventh and eight are related to the shape of the first pulse. The eighth says specifically that a third of the registers covering the first 100 msec (not a third of the time because the register time

interval is not constant) have amplitudes within the first thirty-two range sensitivity steps below the first maximum value and serves as a check that the first peak is not too irregular in shape. The seventh specifically checks that fewer than 36% of the registers before 100 msec are within any one sensitivity range which would make the pulse too flat. The ninth specifies that the second peak must start before 1800 msec (time sample #396) whereas discriminants 5 and 6 would specify that the second peak must occur before 2000 msec. The ninth would therefore appear to be redundant at present but, as with the first, could be modified to increase the NBDS discriminant capability in the future. While the eighth insures that the first pulse had a significant number of registers with an acceptable amplitude, the tenth checks that the pulse is also not too uniform or flat. The eleventh and twelth are designed to exclude lightning flashes which have a smaller second maximum in relation to the first maximum than a nuclear burst and, due to the elongated geometry of the source, cool rapidly to provide a narrow second pulse.

The determination of whether or not the burst is a ground burst is based on the definition of a ground burst as one whose fireball intercepts the surface of the earth. Such an occurrence has at least two effects. First, the fireball will cool more rapidly as it heats the ground and second, the fireball will never reach a second maximum as high as it otherwise would. These two points are addressed by the Ground Burst Discriminants

1) $t_{2max} \leq 9.5916 \times t_{min}$

and/or

2) Second max $\leq$ 1.8018 x First max

III OPTICAL PULSE SIMULATION TECHNIQUES

Simulation techniques based on thermochemical generators will be discussed. Theoretical arguments for the general scaling laws found to hold in the reactions studied to date show that the output and time duration of the pulse can be varied within limits. Contrasts with other sources show that flash lamps also hold promise for providing at least part of the required optical signature. Optical enhancement of the output of any omnidirectional radiating source may prove to be cost effective in field tests. Detailed understanding of the internal mechanisms of fireball development promises additional ways to tailor the output pulse of the generator.

III.1 General Background

No device exists at present that has been used successfully to simulate nuclear pulses to NBDS detectors, although accidental triggering of NBDS due to naturally occurring "superlightning" has been reported. The use of a thermochemical generator based on a metallic oxidization reaction has been proposed as a calibration technique. A brief review of its operation will be presented. Consider the metallic oxidization reaction:

$$M + aO_2 \longrightarrow MO_{2a} + \text{heat}$$

The highest final temperature practically obtainable due to this reaction is that of the vaporization temperature (T_r) of the oxide MO_{2a}, since above this temperature latent heat effects would dominate. Experience has shown that if the reaction can be initiated either at T_r or the lower melting point temperature it will self-sustain at T_r. A thermochemical flash generator is most radiation efficient when there is a large surface to volume ratio, a high temperature T_r, and a sufficient optical density of the reaction products. Thus a system of metallic dust or fine wires mixed with oxygen, and ignited simultaneously at many locations is preferred.

The initial energy is supplied in chemical form by the fuel (M and O_2). The optical fluence is then proportional to W, the weight of M, if sufficient O_2 for reaction is assumed. The

optical flux per unit area of the reacting system (a fireball) is governed by the blackbody equation if the system is optically thick. Thus total radiant heat loss is proportional to T^{4*} and area. If T is constrained to T_r, then the total flux of radiation, $\dot{Q}$, is proportional to the square of the system radius. If the fuel consumption rate exceeds the ability of the system to radiate, the system will expand, losing energy proportional to the time rate of change of the radius. When radiation equilibrium is established the volumetric expansion will cease although the apparent size may increase due to buoyancy effects and local turbulence at the fireball edge.

Since the energy loss in expansion is proportional to volume it can be stated that the stabilized fireball radius will be proportional to $W^{1/3}$. Consequently, since Q is proportional to W, and $\dot{Q}$ to area ($\sim W^{2/3}$), the characteristic time <t> of the optical output is proportional to $W^{1/3}$, assuming a constant radiation temperature, optically dense reaction products, and ignition and burning times less than the characteristic time.

Two distinct types of thermochemical generation schemes are possible. The entire amount of fuel ($M + O_2$) may be ignited at once, or M may be metered into the O_2 volume after initial ignition. Recall that M is in the form of a fine powder, facilitating its injection. In the latter case the additional fuel will have varying effects, instantaneous flux will be lower due to the absorption of energy in raising the fuel to ignition temperature; however, the reaction time may be lengthened arbitrarily, and the expansion of the fireball controlled by the proper metering of fuel.

In summary the key considerations for a thermochemical generator are:

- Choice of the metallic system MO_{2a} on the basis of evolved heat and vaporization temperature
- Choice of the scale of the reaction W
- Choice of the metering rate of fuel, including ignition of all fuel at initiation.

*A silicon dector response cutoff at 1.1 μm causes a loss of the infrared tail so that T^5 is a better estimate of the detected or passed power.

The investigation of the reaction system will follow these considerations.

A review of selected thermochemical reactants was made in Reference 1 and is reported in Table 2.

III.2 Comparison of Thermochemical Pulse With Nuclear Pulse

Reference 1 reports on the current status of the SAI developed thermochemical generator. The following are typical parameters for the largest unit fielded as of March 1977:

$$P_{max} = 10^9 \text{ watts} = 2.4 \times 10^8 \text{ cal/sec} \qquad \text{III.A}$$

$$E_{total} = 1.1 \times 10^7 \text{ cal} \qquad \text{III.B}$$

$$t_{max} = 10 \text{ to } 50 \text{ msec} \qquad \text{III.C}$$

Assuming an isotropic radiation distribution the sensor must be at a range of no greater than 224 km to satisfy microprocessor discriminant number 1. The "generator" has no first maximum, of course; and, thus, the other criteria cannot be met at present with a single unit. With a single reaction the pulse shape of a typical unit will simulate that of the second maximum of a small yield device, or that of the first maximum of a large yield device.

Leaving aside questions of the double pulse device, we wish to estimate the "nuclear equivalence" of the pulse. First, let us assume the pulse is the main or second pulse. A typical thermochemical pulse is of 10 to 50 msec duration to peak, with the shape controllable to some extent. Inverting the familiar relationship

$$t_{max} = 32\ W(KT)^{1/2} \text{ msec} \qquad \text{III.D}$$

Table 2

Energy Release of Selected Thermochemical Reaction Mixtures

COMPOSITION	PARTICLE	HEAT OF REACTION kcal/g	HEAT OF REACTION cal/ccO_2	APPROXIMATE FLAME TEMPERATURE (^oK)
Solid-Gas				
Al + O_2	Al_2O_3	7.4[a]	11.1	3900
Zr + O_2	ZrO_2	2.9[a]	10.8	4400
Mg + O_2	MgO	5.9[a]	12.0	3100
Fe + O_2	FeO, Fe_3O_4	1.6[a]	5.6	-
Ti + O_2	TiO_2	4.7[a]	9.4	-
Be + O_2	BeO	15.9[a]	11.9	-
B + O_2	B_2O_3	14.0[a]	8.4	-
Gaseous				
Al $(CH_3)_3$ + O_2	Al_2O_3	-	4.6	-
Propane + O_2	-	-	3.3	-
Solid				
Al + $LiClO_4$	Al_2O_3	3.0	7,655[b]	3900

[a]Based on weight of metal fuel.

[b]Solid mixture, cal/cc.

and solving for W yields:

$$W(KT) = \frac{t_{max}(msec)^2}{32} \qquad \text{III.E}$$

$$W = 0.1 \text{ to } 2.4 \text{ KT}$$

for the range of t_{max} specified by III.C.

Another method of calculating the yield would be to note that, of the 10^{12} cal/KT released by a nuclear device, a third of the energy is typically thermal and most of this (>0.95) appears in the second pulse. Then III.B leads to:

$$W = 3 \times 10^{-5} KT.$$

Finally, the relation between the peak flux for the second maximum and fluence is:

$$P_{max} \approx 4 \times 10^{12} W^{1/2} \text{ cal} \qquad \text{III.F}$$

and using III.A we find

$$W \approx \frac{1}{4} \times 10^{-8} \text{ KT}$$

Thus, the pulse width, peak power, and total energy of the optical output of the simulator are not consistent yield indicators for a nuclear weapon. Yield equivalents, depending on method of calculation, range from 2×10^{-9} KT to 2.4 KT. Methods of enhancement that direct more flux toward the sensor than that obtained from a radiating fireball would be required to bring these values into synchronism. Additional tailoring of the pulse shape may also be required to simultaneously match the constraints if such consistency is to be demanded by an NBDS system.

On the other hand, if we assume the simulator is employed for the first maximum then:

$$P_{1max} \approx 4 \times 10^{-10} W^{1/2} \qquad \text{III.G}$$

$$t_{min} = 2.5 \times 10^{-3} W^{1/2} \qquad \text{III.H}$$

$$t_{1max} = 2 \times 10^{-4} W^{1/4} \qquad \text{III.J}$$

and are appropriate for use with the information in III.A and III.C.

We then obtain

$$W \approx \frac{1}{4} \times 10^{-4} \text{ KT}$$

$$W \approx 2500 \text{ KT}$$

and

$$W \approx 10^{4} \text{ KT}$$

respectively. And we once again find a range of values for W which covers almost a factor of 10^9.

The overall conclusion is that a source for a supplemental pulse is needed. This may be a fast rising pulse to simulate first maximum, or a very long high intensity source to simulate second maximum. The supplemental pulse may be from a revised version of the thermochemical reaction system or from a different source.

III.3 Review of Potential Optical Sources for the Second Pulse

An initial review of potential sources for the supplemental pulse has been conducted. The following candidates were considered:

Black Body

a) Thermochemical

- Al/O_2
- Zr/O_2
- Others

b) Shock Radiation

- Cylindrical - in O_2 or Air
  - in Argon

- Supercritical shocks by seeding a gas with an optically thick medium
- Multiple interacting shocks
- Implosions

Quasi Block Body

Flash Lamps - Xenon

- Pulsed
- CW

Line Radiation

Lasers

- Pulsed
- Modulated

Hybrids

For the thermochemical generator to be successfully modified, theoretical investigation of its performance is required; this is the main subject of this effort. A variety of metals may be considered. Zirconium has a higher flame temperature and, thus, may produce a brighter output (see Reference 1, page 9 et seg.). Shock radiation, possibly a by-product of the ignition sequence, may be a potential source. Seeding of the shocked medium to increase radiant output is possible.

Flash lamps seem to offer the next great promise in terms of pulse shaping and brightness. They were selected for further investigation as a back-up to the thermochemical system. Lasers seem unsuitable in comparison.

The sources listed above differ in source characterization, size and brightness. To assess the desirability of potential sources, some considerations of optical transmission to a distant detector were made for two cases, a hot radiating ball and a small flash source with optical enhancement in the propagation direction.

In the first case:

$$P_{detector} \propto T^4\left(\frac{r}{R}\right)^4$$

when T is the temperature of an assumed black body ball of radius r, radiating isotropically to a detector at R.

The second case is approximated by a flash source of size r_o, at the focus of an #f = 1 parabolic mirror of radius r'. The object size is r' + R sinα, when $\alpha \approx r_o/r'$. For large R this reduces to

$$P_{detector} \propto T^4\left(\frac{r'}{R}\right)^2$$

If we assume that the size of the first fireball is equal to that of an #f = 1 parabola then the relative advantage is the ratio of the source temperatures to the fourth power. Since structural supports are built in the first case to approximately the fireball dimensions, and in the second to the size of the parabola, an assumption of equal costs is justified. A much more detailed cost/benefit analysis will have to be made eventually, but this first look indicates that a small thermo-chemical source, a flash lamp or other small source enhanced with optics may be potentially useful. A second result of this calculation is to indicate the relative worth of optical enhancement with any source.

III.4 Details of Flash Lamp Systems

A brief review of flash lamp systems was made in order to obtain comparative information for analysis of cost benefit. Typical linear or helical quartz tube flash lamp characteristics depend mainly on excitation energy. Designs of up to 1m in length and 2 cm in diameter are standard. Typical noble gas filling pressures range between 0.2 and 1.0 atmosphere, with Xenon, Krypton and Argon being the most commonly used elements. Water or gas cooling may be provided, or natural air cooling used if repetition rates are not severe. Typical parameters for large (1m long) flashlamps are color temperature up to 9400^{o}K, high

emissivity, particularly at longer wavelengths, and costs of about $300 to $600 in quantity purchase. Such lamps are approximately 50% optically efficient, based on electrical input, and may be cycled many thousands of times if not run near peak output. Rough cost estimates indicate about $10K per module (in quantity purchase), including power support for a 4000 cal/pulse optical output.

IV COMPARISON OF THEORY TO TEST DATA - THERMOCHEMICAL GENERATOR

The general theoretical arguments for fireball ignition and development are compared with three sets of test data on thermochemical reaction tests. The first series of fairly large explosively ignited tests show good agreement with the theoretical predictions. A second set of small scale test data is then used to confirm this over a wider range of parameters.

IV.1 Test Data Taken Prior to March, 1977

In this section we review the salient test data of Reference 1 for comparison to theoretical arguments developed above. We discuss initially the comparison with the general conclusions, then refer to quantitative comparison of theory with experiment.

From the general conclusions (Section 5, Ref. 1) we note:

a) Fluence scales linearly with the weight of aluminum, (all other parameter ratios being held constant) in agreement with the basic equation for the device.

b) Peak flux scales linearly with the weight of aluminum implying small variation in the fundamental output pulse width over the range of aluminum weights studied. Since the larger tests were made up of smaller models fired simultaneously, this is not surprising. Later work over a wider range of aluminum weights more clearly revealed the $W^{1/3}$ dependency of pulse width.

c) Shock effect proportional to output was noted. The shock source is postulated to be the primacord igniter. Since this is proportional to output in the modular scheme used, the results follow.

d) Fireball radius is found to be proportional to $W^{1/3}$, where W is the weight of aluminum powder. This is consistent with a fraction of the fireball energy being dissipated in fireball expansion. This fact is corroborated by the relative radiative efficiency

(~10%). Modularity of the test devices also would tend to produce the effect.

e) The peak fireball temperature of about $3600^{o}K$ is consistent with that of the vaporization temperature of alumina (Al_2O_3) while the temperature at fireball expansion stabilization ($2400^{o}K$) is consistent with the alumina freezing point.

Analysis of fireball data in Reference 1 evolved three empirical scaling laws, for fireball radius at stabilization,

$$r_f(m) = 2.5 \ W(Kg)^{1/3}$$

for the time of fireball stabilization,

$$t_f(sec) = W(Kg)^{1/3}/16$$

and for fireball radius as a function of time to stabilization

$$r(m) = 5 \ (W(Kg) \ t(sec))^{1/4}$$

An average optical efficiency for the fireball of 10^3 cal/gmAl was measured. Eight shots of sizes from 0.5 gm to nearly 15 Kg were used to calculate these values.

IV.2 Test Data on Small Scale Shots

Over 100 small scale shots of thermochemical reaction systems using a variety of configurations have been reported.[2] Since the optical output was detected with a single photodiode and not corrected for fireball size or temperature effects, only a very limited amount of information can be drawn from these tests. Since these tests and the previous series cover a fairly wide range of aluminum weight, investigation of optical pulse duration scaling can be made. In addition, since the upper limit of particle size was specified, search for particle size effects may be made. However, since the particle size distribution is unknown, and since several different grades of powder were employed, no firm conclusions can be drawn. In any case, about 40 small scale tests using

explosive ignition were studied for pulse length effects. Of these, about 1/4 (11/41) were duds and were ignored in the analysis. The average pulse widths for the remaining tests are plotted on Figure 6 where data from 6, 18 and 60 micron upper limit (of 5 gm aluminum weight) particle diameter tests are indicated separately along with a typical error. In addition, tests at 100 gm weight are indicated individually. Pulse widths from the larger shots performed in the first test sequence are plotted also. Despite considerable data scatter the general $W^{1/3}$ trend seems well verified. The data scatter may be due to the variety of aluminum powders and other experimental variables or to the lack of instrument corrections.

Investigation of the balance between the fundamental expansion time of the fireball with the ignition and burning times of the particles, and of the optical thickness of the fireball indicate allowed regions of reaction parameters. As an example of this analysis consider the interplay of particle ignition plus burn with fireball expansion to peak output (at $3000^{o}K$). From Appendix A we derive on general grounds (Eq. L)

$$t_p(\text{sec}) = 0.0063\ (W(\text{kg}))^{1/3}$$

and that the particle ignition time is given by, Eq. U,

$$t_i(\text{sec}) = 2.5 \times 10^{-6}\ (a(\mu))^2$$

while burning time is given as, Eq. V,

$$t_B\ (\text{sec}) = 0.0002\ a(\mu) - .0004$$

Equating the numerical value of the expressions for ignition plus burning with expansion to peak output yields the constraint equation

$$a(\mu) = (2.52 \times 10^3\ (W(\text{kg}))^{1/3} + 1760)^{1/2} - 40$$

This formula is evaluated in Table 3.

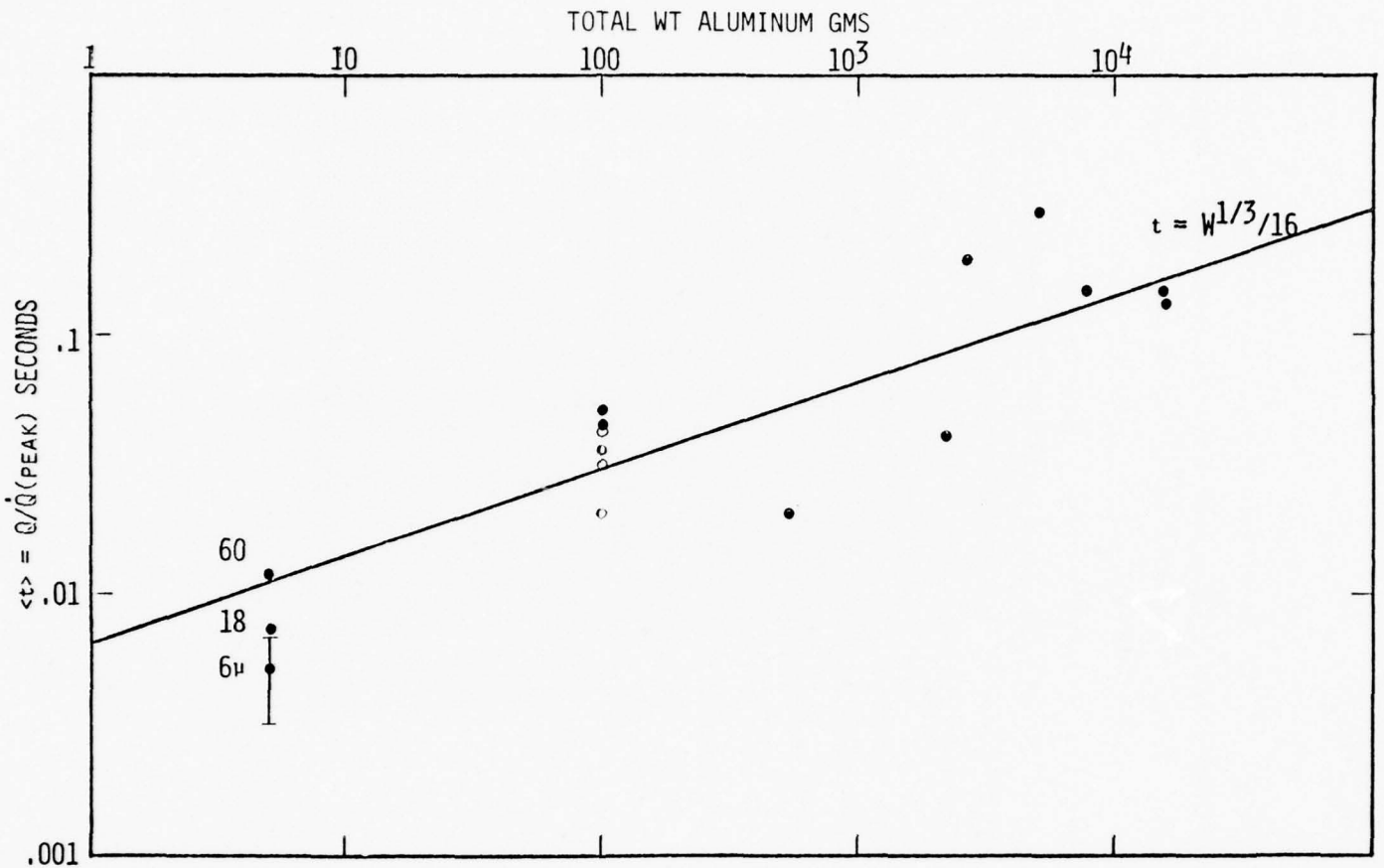

Figure 6. Pulse Widths as a Function of Aluminum Weight

Table 3

Evaluation of the Constraint that Particles Must Ignite and Burn in the Characteristic Expansion Time of the Fireball

W(kg)	a(μ)
0	2.0
0.0001	3.3
0.001	4.9
0.01	8.0
0.1	14.0
1.0	25.0
10.0	45.0
100.00	76.0

Likewise another constraint equation can be derived by requiring that the fireball radius at stabilization be one mean free path thick or:

$$R_0 = \ell_0$$

Using equations derived in the Appendix we obtain

$$a(\mu) = 23(W(kg))^{1/3}$$

These two constraints are indicated on Figure 7 along with specific points indicating parametric location of tests conducted to date. Tests far from the criteria tended to have lower efficiency than those on or near the criteria. Tests where the characteristic time for fireball expansion is much less than that required for ignition and burning tended to be less efficient than one might expect. In the extreme opposite case the tests also show reduced radiation efficiency. This may be due to the fact that more rapid ignition and burning drives the expansion and decreases radiation efficiency.

IV.3 Additional Test Data

The most recent series of tests performed by J. Dishon (Reference 2) have consisted mostly of shots using a configuration of pre-mixed aluminum with oxygen. This set-up is also capable of injecting additional aluminum into an ignited fireball.

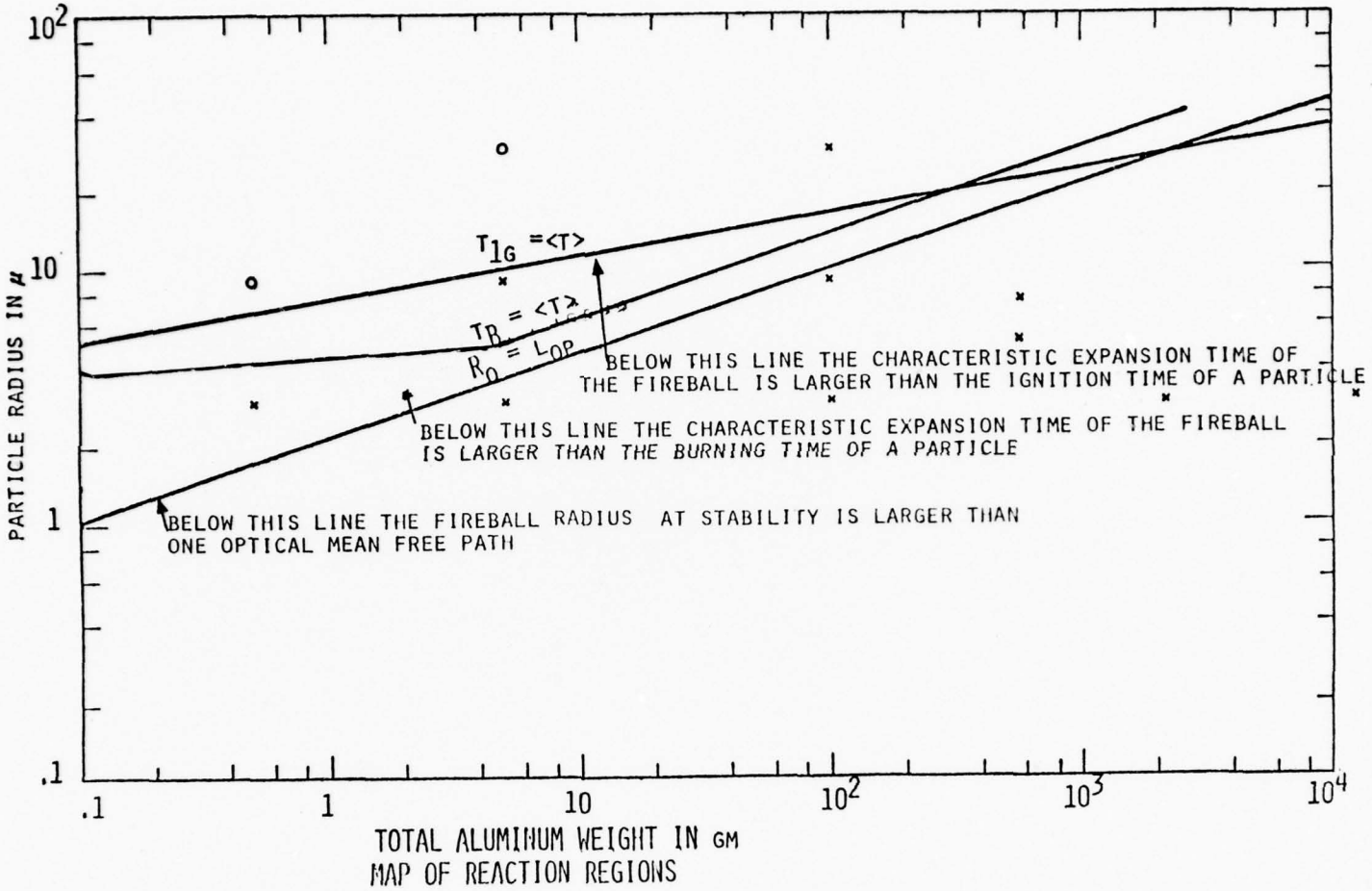

Figure 7. Constraint Equations

In the case of the pre-mixed system an optically thin mixture is desirable for longer pulse duration and the opposite is true for a shorter pulse. In the case of an optically thinner mixture, higher optical efficiency is anticipated due to the more effective radiation from within. In optically thicker mixtures expansion competes with radiation, lowering optical efficiency. Table 4 summarizes the qualitative features of several test configurations and indicates the expected scaling laws. References 5 and 6 summarize NBDS data obtained in these tests.

Table 5 reports scaled fluence as a function of oxygen to aluminum ratio and particle size for metered flow conditions (System C of reference 2). This illustrates the data trends to decreasing efficiency with particle size. These data indicate average fluences of 2000 to 3000 cal/gm are attainable.

Table 4

Test Configuration Summary

TECHNIQUE	OPTICAL CONDITIONS	DUST A/V RATIO	SCALING
Explosive ignition of Al, drived into O_2	Dense to enhance radiation over expansion	Large to promote ignition	$Q \sim W$ $\dot{Q} \sim W^{2/3}$
Pyrotechnic ignition of homogeneous Al - O_2 mixture	Thin to improve radiation efficiency and lengthen pulse	Particle size helps control burn rate	$Q \sim W$ $\dot{Q} \sim \frac{1}{\rho_{dust}}$
Metered flow of Al into ignited fireball in O_2	Dense	Large	$Q \sim W$ $\dot{Q} \sim$ flow

Table 5

Scaled Total Fluence Outputs of Various Laboratory-Scale TRS Designs

Scaled Total Fluence (cal/gm)	Mixing Technique	O_2/Al	Al Particle Size (μ)
3354	C	7.8	6
3200	C	7.8	18
2274	C	5.1	6
2081	C	5.1	18
1767	C	5.1	60
1500	C	7.8	60

V SUMMARY AND RECOMMENDATIONS

While a detailed theory concerning thermochemical reactions (TCRs) is not available at the present time, the basic laws of physics seem to be sufficient to explain the gross observables such as time to fireball stabilization, stabilization radius, expansion energies and energy radiated as a thermal pulse. For many applications of TCRs, this level of information is sufficient.

For the present problem, however, more detail is necessary. The time history of the thermal pulse and its spectrum must be predictable at least to a point where the variables of fuel type, fuel-oxygen mix, initial fuel charge and fuel feed rate can be approximately determined before a test series is begun. It is felt, at this time, that this level of detail will be achievable with a more refined theory, possibly including a computer model for fireball development, and data which should soon be available if testing is continued.

At the conclusion of this investigation the following statements summarize the state of knowledge concerning large scale optical flash sources:

1) Nuclear waveforms are not directly simulated by any other source. Their unique two peaked shape (time spectra) and intensity of output are responsible for this.
2) The three most promising sources of optical flash appear to be the SAI developed thermochemical generator (although not necessarily using aluminum solely), a high intensity flash lamp bank, and shock heated air or argon.
3) In order to create the double peaked time spectra two sources, fired in rapid succession, will be required. Each source will have different properties to properly simulate the first and second maxima.

4) In order to bring peak flux, fluence and rise time at a distant detector into the proper yield relationship, considerable "tailoring" of the sources is required. A first order calculation of the effect of source size indicated that the use of reflector panels to augment a small source may be as effective as creating a large source. A more detailed cost/benefit tradeoff study will be required. Freeing the source size (to first order) in design may allow more readily attainable pulse parameters.

5) Concerning the SAI developed thermochemical optical pulse generation technique itself, we have verified that the prima-cord is both the probable ignition source, and the cause of most of the shock output. Reduction in prima-cord loading may prove advantageous. The chemical reaction is ignited above 2400°K (the melting point of Al_2O_3) and burns initially at 3600°K decaying to 2400°K at about 100 msec. At this point, the fireball is well stabilized and optical radiation is relatively unimportant to growth dynamics. The energy budget calculation at this stage of development shows that of the initial energy, 20 percent goes to fireball expansion, 70 percent to residual fireball sensible heat, and 10 percent to radiation.

6) The fireball density of both dust and gas are calculated as a function of time. At stabilization the fireball gas density is about 10 percent of normal atmospheric density and the dust loading is 10 percent of gas density.

For the tests conducted prior to 1 March 1977, the fireball is always optically dense, but decreasingly so as it evolves. At stabilization it is three mean paths in diameter.

The radiative cooling rate calculated on the basis of a uniformly heated sphere is consistent with measurement. Some additional cooling due to convective effects seems to be present.

7) The single theory proposed has been found to agree quite well with the results of a much larger data base than that provided by the fireball tests run by SAI so far; that of the fireballs produced by rocket propellants. The accompanying figures (5 and 6 from Reference 5) reproduce some data on propellant fireballs and include points for some of the smaller SAI thermochemical reactions (fuel weights < 5 pounds in Figure 5 and < 50 pounds in Figure 6). The points are very close to the line extrapolated from previous data in the first case while in the second the slope of the line for the thermochemical reactions is about the same as that for the rocket fuel case. Since the rocket fuel stabilizes at a lower temperature than the aluminum used in the SAI tests the intercept differences are expected.

8) At this time it appears possible to do some thermal pulse shaping by controlled injection of a metal powder fuel into the fireball after initiation. The paucity of data on such reactions has precluded a theoretical prediction of the effects such a procedure might produce however. It would therefore appear to be advantageous to design and test such a device.

9) Scaling laws evolved in the text hold to within a factor of two over a region 0.5 to 20,000 gm of aluminum. The pulse duration for an explosively ignited device is predictable from the scaling laws. Durations of the order of 100 msec seem feasible. Additional scaling laws based on ignition of premixed aluminum-oxygen systems indicate higher radiant efficiencies and longer burning times are probable. Considerable tailoring of pulse duration seems possible.

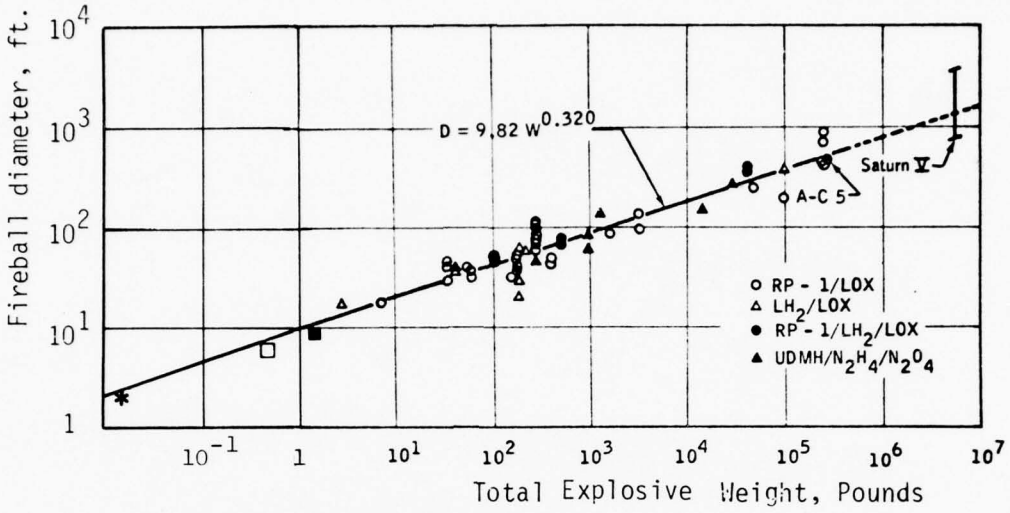

Figure 8. Fireball Diameters

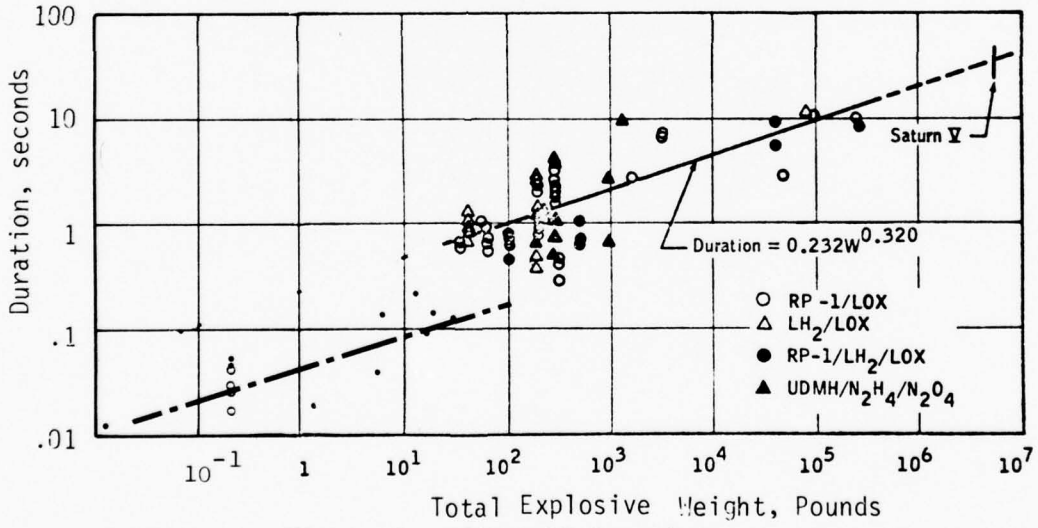

Figure 9. Fireball Durations

10) Continued work is required to finalize these conclusions, as is noted above in the area of improved nuclear waveform and triggering requirements for NBDS. More detailed review of the time history of the multiple thermochemical tests data is required, and a thorough review of the small scale test is warranted. Completion of a detailed source augmentation cost/benefit study should be accomplished. A detailed thermochemical reaction calculation including collective effects should be performed. Other particle types (magnesium is a prime candidate) ought to be considered.

11) The development of an effective and inexpensive NBDS simulation is now within the range of technical feasibility. Design equations and scaling laws have been developed in this report for thermochemical reactions based on aluminum and oxygen fuels. These coupled with the NBDS trigger requirements allow prediction of thermochemical optical pulse generators parameters that simulate nuclear weapon output. A detailed study of the thermochemical reaction process leading to optical pulse output is given in the appendix.

APPENDIX A

A. THEORETICAL ANALYSIS OF THERMOCHEMICAL FLASH GENERATION

Prediction of the behavior of the thermochemical generator will be based on a detailed understanding of the physical and chemical processes that make up fireball development. Particle ignition and burning rates may control fireball development and radiation efficiency. Fireball growth consumes energy and allows increased radiation. The details of individual particle interaction help to control output power and duration.

A.1 Overall Models

In general, the theoretical knowledge to completely specify the phenomenon of thermochemical flash generation via the SAI-developed optical flash unit is imperfect. Considerable data exist, but there is not yet a coherent theoretical base to support future development of specific tailored pulse output devices. It is the purpose of this section to describe theoretical models of thermochemical flash generators. Two models will be developed. The first is a general model of fireball development that will be useful for scaling. The second type treats each specific phase of the fireball development in detail and forms the basis of a detailed model of the fireball thermodynamic development. The second model may be useful for detailed tailoring of the output features of flash generators.

The fundamental chemical reaction of burning aluminum is:

$$2\ Al + \frac{3}{2}\ O_2 \rightarrow Al_2O_3 + 7400\ cal/gm\ al$$

Some of the physical properties of Al and Al_2O_3 are contained in Table A-1.

Table A-1

PHYSICAL PROPERTIES

	Temperature		Latent Heat		
	Melting	Boiling	Fusion	Vaporization	Density
Al	932°K	2740°K	94 cal/gm	2619 cal/gm	2.70
Al_2O_3	2318°K	3800°K	244 cal/gm	--	3.99

Single aluminum particle ignition temperatures in air are measured to be about 2300°K, approximately the melting point of alumina (Al_2O_3). Some controversy exists as to whether the reaction will proceed at lower temperatures in dust clouds due to cooperative effects.

The general fireball model starts from basic physical principles to develop the thermodynamic relations for fireball size, duration and growth. Assume that W kilograms of fuel are available, and at t = 0 are ignited. The thermochemical reaction is initiated at the melting point of Al_2O_3 ($\sim$2300°K), when the elemental aluminum is free to react with the oxygen, and rapidly progresses to the vaporization temperature of Al_2O_3 ($\sim$3800°K). The reaction products are assumed to be gaseous regardless of the initial state of the fuel and to remain so, obeying the ideal gas law, until cloud stabilization. In an unconfined system, we can take the pressure on the gas to be constant at p_o, atmospheric pressure, so that the gas law takes the form of

$$\frac{V_f}{N_f T_f} = \frac{V_i}{N_i T_i}$$

or

$$V_f = \frac{N_f}{N_i} \frac{T_f}{T_i} Vi \qquad (A)$$

where $\frac{N_f}{N_i}$ is the molar ratio of the gaseous product to the gaseous reactant (i.e., 1 mole of Al_2O_3 to 1.5 moles of O_2) and $\frac{T_f}{T_i}$ is the ratio of the final gas temperature to the initial gas temperature (290°K).

The initial gas volume can be determined by noting that 0.88 grams of O_2 combine with each gram of Al to produce Al_2O_3, and that at standard temperature and pressure 32 grams of O_2, in a pure gas form, has a volume of 22.4 liters.

We then find that, in MKS units,

$$V_i = .616\ W$$

where W is the weight of the aluminum.

So that

$$V_f = 1.42 \times 10^{-3}\ T_f\ W$$

and

$$r_f = .070\ T_f^{1/3}\ W^{1/3} = C\ T_f^{1/3}\ W^{1/3} \qquad (B)$$

$$= .937\ W^{1/3} \text{ at } T_f = 2400^{o}K$$

Support for this simple model comes from High, who reviewed data for about 60 fireball radii produced by rocket propellant ignitions over a range from 1 Kg to almost 10^6 Kg. He found*

$$r_f(m) = 1.16\ W^{0.32} \text{at } T_f = 2400^{o}K$$

(see Figure A-1 taken from Reference 7). The constant of proportionality is, of course, fuel dependent which may explain the difference between the two results.

The simple model can also predict fireball durations if we assume that the optical output versus time is triangular, and define the duration as the time between half power points. Then the relationship between optical output (Q), peak radiant flux per unit area ($\dot{Q}$), area (A), and time duration (t) is:

$$Q = \dot{Q}AT = dW \qquad (C)$$

where d is the optical output per unit weight of Al (in cal/Kg).

*Within the error of the figure and when expressed in MKS units

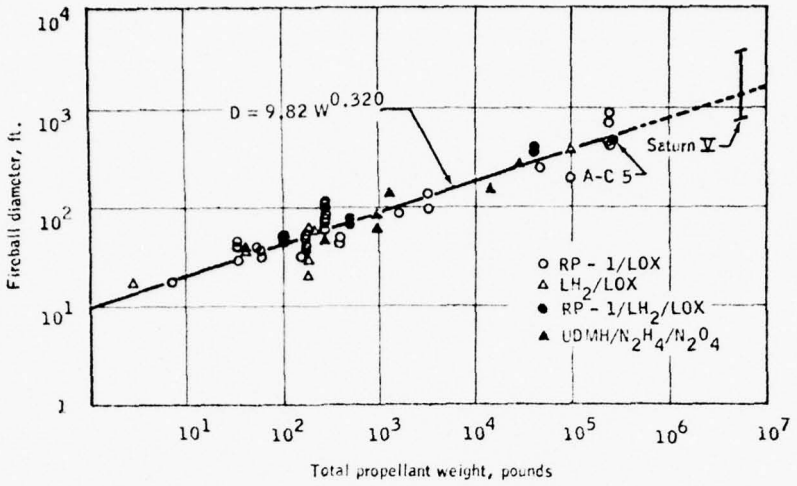

Figure A-1. Fireball Diameters for Various Weights and Types of Propellants.

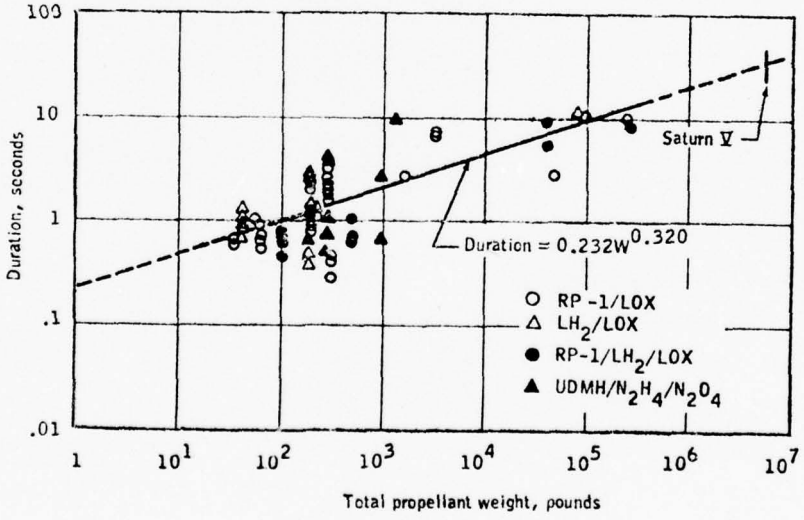

Figure A-2. Fireball Duration for Various Weights and Types of Propellants.

Peak flux per unit area (assuming radiation dominates) is given by:

$$\dot{Q} = \sigma E(T_f^4 - T_1^4) \qquad (D)$$

where

$$\sigma = 1.36 \times 10^{-8} \text{ cal/m}^2 \text{ sec } {}^{o}K$$

and E = fireball emissivity.

Then from Equations C and B, we find

$$t = \frac{\alpha W^{1/3}}{4\pi\sigma E C^2 (T_f^4 - T_i^4) T_f^{2/3}} \qquad (E)$$

C being .070 from Equation B, and that

$$t = dW^{1/3} \qquad (F)$$

In evaluation, t, C, and possibly E may be functions of T_f in addition to the explicit T_f dependency shown. This in essence indicates that t, the fireball duration, will be a function of the cube root of the weight of fuel. Reference 5 again provides data on time duration. Using the value of $2400^{o}K$ for T_f as a suitable average for the test conditions under which data was taken, and a value for α of 10^6 cal/Kg and E = 1 as representative of the fireball emissivity for these fuels and C as indicated above, we thus obtain

$$t(\text{sec}) = 0.201 \quad W(\text{Kg})^{1/3} \qquad (G)$$

while High finds that, for rocket fuels with $T_F = 1800\ {}^{o}K$

$$t(\text{sec}) = 0.180 \quad W(\text{Kg})^{0.32}$$

for a series of about 60 fireball tests. Figure A-2 illustrates his results from empirical data fitting. Table A-2 gives values of the coefficient d and the final temperature for the aluminum fuel case.

The final stage of development of the model is to convert from a static to a time dependent or growth model. This is accomplished by dimensional analysis. The expression for the time duration, Eq. G is also true for any instant of time, where W is changed

Table A-2

Evaluation of

$t(sec) = d \; W(Kg)^{1/3}$

As a Function of Final Temperature

d	T_f (^oK)
0.0302	3600
0.201	2400
0.470	2000
0.769	1800

to the fuel consumed up to time t. The general equation for fireball radius growth is then a function of fuel weight and time

$$r = f(W,t)$$

If we assume

$$r = \gamma W^{\alpha} t^{\beta}$$

and use equations B and E and keep T constant then

$$CW^{1/3} = \gamma d^{\beta} W^{(\alpha+\beta/3)}$$

implying $\alpha + \beta/3 \approx 1/3$

While this defines a set $\{\alpha, \beta\}$ for which the equation may be valid, the simplest member of the set with non-zero positive values will be taken, so that

$$\alpha = \beta = 1/4$$

and $$r = \gamma (Wt)^{1/4} \qquad (H)$$

with $$\gamma = C/d^{\beta}$$

No data from reactions other than the Al_2O_3 system were available to test this model. The agreement between the growth model values

$$r_f(m) = 2.6\ (W(Kg)t(sec))^{1/4},\ T_f = 3600^{o}\ K$$

$$r_f(m) = 1.4\ (W(Kg)t(sec))^{1/4},\ T_f = 2400^{o}\ K$$

and the data is acceptable.

A.2 Detailed Fireball Development Model

Basically, the Flashbulb reaction has two distinct phases: the prima-cord detonation phase, and the Al/O_2 reaction phase. At t = 0 the prima-cord is ignited, sending a shock wave through the aluminum powder tube, the O_2 bag and into air in the matter of about 1 msec. The shock heated and dispersed powder is accelerated in the outward flow field and immediately encounters shock heated O_2. The outer edge of the expanding dust layer is ignited by this. The core

area may ignite also due to the residual hot products of the prima-cord. In any case the dust layer is optically thick and the surface radiation is as from a black body. By t = 1 msec the glowing dust layer is visible in high speed photography. The layer expands due to drag in the outward flow of shocked air, and due to thermodynamic expansion. Radial stabilization occurs because of the consumption of O_2 within the fireball. Specific calculations of the following effects were attempted:

- Prima-cord shock trajectory
- Prima-cord shock velocity
- Shock overpressure
- Shocked air temperature
- Fireball trajectory
- Fireball density
- Optical thickness in the Fireball
- Thermodynamic expansion
- Radial stabilization, cooling

A.3 Shock Model

For the shock trajectory we used the results of Jones, Goyer and Plooster[8], who show that for a 25 grain prima-cord the shock trajectory, t(r), can be written as

$$t(r) = 1.27\ [(1 + 5.67 \times 10^{-4}\ r^2)^{1/2} - 1]\ \text{msec}$$

where r in cm is the radius of the shock front at time t.

Jones et al., give a formula for the overpressure correct in the weak shock limit as:

$$\Delta p = \frac{7.7}{(1 + 5.8 \cdot 10^{-4} r^2)^{3/8} - 1}\ \text{psi}$$

We also used the approximate formula

$$\frac{P_2}{P_1} = 1.166\ M_1^2 - 0.166$$

for the pressure ratio across a strong shock in air, when M_1 is the Mach number in the undisturbed region ahead of the shock. Generally, these agreed fairly well.

The temperature ratio of shocked to undisturbed air was estimated as

$$\frac{T_2}{T_1} \simeq .2M_1^2$$

This is strictly valid only for strong shocks (M_1 large) and indicates that the shock wave is sufficient to ignite the Al,O_2 mixture.

A.4 Fireball Parameters (radius as a function of time)

The fireball trajectory was obtained empirically by measurement from high speed photography of several Flashbulb shots. As explained in A.1, these agreed with the simple gas expansion model. Fireball density was calculated assuming isotropic dust distribution. Reference 1 data for a variety of shots allows a formulation of radius of fireball vs. time to be made and is used directly here. From this, fireball dust density and optical thickness can be found.

Fireball gas density is estimated from the perfect gas laws given the measured fireball temperature.

The comparison of the detailed quantitative results of Reference 1 will now be made. The first general area to be covered will be radiative energy transfer. The relationship for fireball stabilized size

$$R_o(m) = 2.5\ (W(kg))^{1/3} \qquad (J)$$

and fireball growth

$$R(m) = 5\ (W(kg)t(sec))^{1/4} \qquad (K)$$

as determined in Reference 1 are found to be in agreement with the overall model for fireball development derived in Section (A.1).

Given the relationship of fireball radius to aluminum weight and time after ignition, the fireball density and optical thickness will now be determined. The above equations imply that the time of fireball radial stabilization is

$$t_o(\text{seconds}) = 0.0625(W(kg))^{1/3} \qquad (L)$$

and the density of the fireball gas, fireball dust and the fireball optical thickness can be calculated.

The fireball gas density is given by the ideal gas law - using the stabilization temperature of 2400^oK

$$\rho_{gas} = .157 \text{ mg/cc, at fireball radial stability}$$

$$\rho_{gas} = .100 \text{ mg/cc at } 3600^oK \text{ at the peak power point}$$

The average dust density at fireball radial stabilization (assuming homogeneous mixing) is given by

$$\rho_{dust} = \frac{\text{Mass of Aluminum}}{\text{Volume of Fireball}}$$

$$\rho_{dust} = \frac{W}{\frac{4}{3}\pi R_o^3} = \frac{1 \text{ Kg}}{\frac{4}{3}\pi(2.5)^3 m^3} = 0.015 \text{ mg/cc at stabilization}$$

$$\rho_{dust}/\rho_{gas} = 0.1 \text{ at stabilization}$$

The dust density as a function of time can be found by application of the fireball growth equation rather than using the radius at stabilization. The more general equation is then

$$\rho_{dust}(t) = \frac{0.0019 \left[W(kg)\right]^{1/4}}{(t(sec))^{3/4}} \left(\frac{mg}{cc}\right)$$

The optical thickness is calculated from the number density per cubic cm., N, and the optical cross section σ, thus

$$\ell_{optical} = \frac{1}{N\sigma}$$

using the number density definition, the average dust density is defined as,

$$\rho_{dust} = N x \rho_{al} x \left(\frac{4}{3}\pi a^3\right)$$

when a is the average particle radius, and ρ_{al} is the density of solid aluminum. Thus,

$$\ell_{optical} = \frac{\rho_{al}\left(\frac{4}{3}\pi a^3\right)}{\rho_{dust}\sigma}$$

where a is the particle radius in cm.

$$\ell_{optical} = \frac{2.7 \frac{gm}{cm^3} \times \frac{4}{3}\pi a^3 cm^3 \times 10^4 \ \mu/cm}{\frac{.0019 \times 10^{-3} W^{1/4}}{t^{3/4}} \left(\frac{gm}{cm^3}\right) 2\pi a^2 cm^2}$$

$$\ell(m) = 0.94 \ a(\mu) \left|t(sec)\right|^{3/4} \left|W(kg)\right|^{-1/4}$$

$\ell = 0.94$ m for $a = 1\mu$, $t = 1$sec.

$= 5.70$ m for $a = 6\mu$, $t = 1$sec

The following table (Table A-3) indicates the values of fireball size, dust density and optical thickness as a function of time for 1 Kg,

Table A-3

APPLICATION OF FIREBALL EQUATIONS
TO CALCULATION OF GROWTH PARAMETERS

CASE: 1 kg Aluminum Powder, 6μ Diameter

TIME (SECONDS)	RADIUS (METERS)	DUST DENSITY (mg/cm^3)	RATIO DUST TO AIR DENSITY	OPTICAL THICKNESS (METERS)	RATIO RADIUS TO OPTICAL THICKNESS
0.001	0.89	0.34	3.4	0.016	56
0.01	1.58	0.06	0.38	0.089	18
0.06	2.50	0.015	0.10	.352	7
0.10	2.81	0.01	0.06	.502	6

ASSUMPTIONS: Homogeneous Fireball at $3600^{o}K$ to 10 msec, $2300^{o}K$ Beyond, Ideal Gas Laws Apply

aluminum dust of 3 micron radius particle size. The cloud is assumed to be at $3600^{o}K$ to after 10^{-2} seconds, and $2300^{o}K$ for 10^{-2} seconds and later. Reference to the table will show that the fireball is always optically thick. For example, it is 12 mean free paths thick at 0.1 seconds well after all significant optical output has ceased. An expression for the ratio of the fireball radius to optical thickness can be derived from the general formula above. The optical thickness at stability is

$$\ell_o(m) = 0.12\ a(\mu)$$

independent of weight of aluminum.

The ratio of fireball radius to optical thickness at stabilization is given by

$$\frac{R_o}{\ell_o} = \frac{21.3(W(kg))^{1/3}}{a(\mu)}$$

Table A-4 shows the results of the evaluation of this formula for a variety of particle sizes and aluminum weights. These tables indicate that under the test conditions of Reference 1 ($a = 3\mu$ $W \geq 500gm$) the fireball is of sufficient optical thickness for good radiation efficiency.

A.5 Fireball Expansion

The second major energy loss mechanism to be studied is that of fireball expansion. The fireball expands because the rate of energy generation exceeds the ability of the surface to radiate. Thus the fireball expands, absorbing energy in thermodynamic work, and increasing the surface to allow more radiation. Stabilization is reached when the rate of generation and loss equalize. The fireball radius is given by equations J and K. The energy absorbed in expansion after initiation is given, in general, by

$$E_e(t) = p_o\ (V_f(t) - V_i) \qquad (M)$$
$$\simeq p_o\ V_f(t)$$

Table A-4

CALCULATION OF THE RATIO OF FIREBALL RADIUS TO OPTICAL THICKNESS AT STABILITY FOR A VARIETY OF CASES

ALUMINUM WEIGHT (gm)	0.5	5.0	100	500	1000	10000	20000
PARTICLE DIAMETER (μ)							
6	0.56	1.21	3.30	5.6	7.1	15.3	19.3
18	0.19	0.40	1.10	1.9	2.4	5.10	6.42
26	0.13	0.28	0.76	1.3	1.64	3.53	4.45
60	0.056	0.12	0.33	0.56	0.71	1.53	1.92

ASSUMPTIONS: Homogeneous Fireball at 2300^{o}K Stabilization Temperature

where p_o = local atmospheric pressure and V_f is the fireball volume at time t. Thus the total energy consumed in expansion to radial stabilization volume V_o is

$$E_{eo} = p_o V_o = 1.57 \times 10^3 \text{ cal/gmA}\ell \tag{N}$$

The expansion energy as a function of time is given by

$$E_e(\text{cal}) = 1.26 \times 10^7 \left| W(\text{kg}) t(\text{sec}) \right|^{3/4} \tag{O}$$

and the power absorbed in expansion is given by

$$P_e(\text{cal/sec}) = \frac{9.45 \times 10^6 \, W(\text{kg})^{3/4}}{t(\text{sec})^{1/4}} \tag{P}$$

while the power loss per unit area is given as

$$P_e(\text{cal/cm}^2\text{sec}) = \frac{3.01 \, (W(\text{kg}))^{1/4}}{(t(\text{sec}))^{3/4}} \tag{Q}$$

The power loss due to expansion is given in Table A-5 for various times and aluminum weights. Since p_r the radiative power per unit area (assuming a black body and unit emissivity) is given by

$$P_r = \sigma T^4 \tag{R}$$

$$\text{with } \sigma = 1.36 \times 10^{-12} \text{ cal/cm}^2\text{sec}^{\circ}\text{K}^4$$

the growth time to the point when radiation and expansion losses (R and Q) equalize is

$$t_B = \left(\frac{3.01}{\sigma T^4}\right)^{4/3} (W(\text{kg}))^{1/3} \tag{S}$$

Table A-5

POWER LOSS FROM EXPANSION PER UNIT AREA OF FIREBALL
FOR VARIOUS ALUMINUM WEIGHTS AND TIME INTERVALS

W(gm)	0.5	5	100	1000	10,000	20,000
T(seconds)						
.001	80	142	301	535	952	1132
.003	35	62	132	234	417	497
.01	14	25	54	95	169	201

A final calculation can be made of the rate of consumption of the aluminum fuel. The output rate is made up of radiative and expansion losses together must equal that of fuel consumption. From

$$\dot{Q}_i = \dot{Q}_r + \dot{Q}_e = \frac{\alpha W}{t_r}$$

where α is the effective value of the fuel ($\sim$3106 cal/kg) and t_r is the net consumption time constant. Then, using Eqs. P and D with the area of the fireball surface, we have

$$\frac{\alpha W}{t_r} = 4\pi\sigma T^4 (5W^{1/4} t^{1/4})^2 + 9.45 \times 10^6 \frac{W^{3/4}}{t^{1/4}}$$

$$\frac{1}{t_r} = 231\left(\frac{t}{W}\right)^{1/2} + 3.04\left(\frac{1}{Wt}\right)^{1/4} \quad \text{at } T = 3600^{o}K$$

Table A-6 lists values of t_r at peak output for various aluminum weights. Also shown is the particle radius a that has the same ignition and burning time, and the rate of consumption of the fuel $\dot{W} = W/t_r$.

Table A-6

Results of Aluminum Consumption Calculation

W kg	t_r sec	a μ	$\dot{W}$ kg/sec
0.001	0.004	13	0.25
0.01	0.008	22	1.25
0.1	0.018	35	5.60
1.0	0.040	55	25.00
10.0	0.080	80	125.00

This particle radius is therefore different from that shown in Table 3 which was determined by the time to fireball peak output rather than the longer time for all radiation output used here.

The thermodynamic expansion of the fireball is calculated via the formula

$$W_{th} = \int_{V_i}^{V_f} pdv = P_{atmos} (V_f - V_i)$$

for the case of expansion of a gas cloud in the atmosphere.

The cooling rate of the fireball is determined by the equation for the rate of energy loss:

$$\frac{4}{3} \pi r^3 \rho c_p \frac{dT}{dt} = \sigma E T^4 \, 4\pi r^2$$

as shown in equation (3), page 14, of Reference 2 which yields

$$\frac{dT}{dt} = \frac{3\sigma E T^4}{r\rho c_p} \qquad (T)$$

where ρ and c_p are the density and the specific heat at constant pressure for the fireball. The cooling rate of a spherical shell would be of similar form but with no 1/r dependency.

The final calculation that will be made here is of the cooling rate of the fireball using Eq T.

$$\frac{dT}{dt} = \frac{3\sigma E T^4}{r\rho c_p}$$

using: $\sigma = 1.36 \times 10^{-12} \frac{cal}{cm^2 sec\, ^oK}$

$E = 1$

$c_p = 6$ cal/mole-^oK

and $\rho fireball = 0.4 g/_{ltr}$ at 2300^oK

we find $\frac{dT}{dt} = 15000 \frac{^oK}{sec}$ at $T = 2300^oK$

A value of about 20000^oK/sec at 2300^oK for fireball cooling was observed. Convective or turbulent heating of the air, test objects and the ground surface could account for the additional cooling.

A.6 Energy Balance

Calculation via energy balance of the total energy radiated per gram of aluminum consumed, up until the stabilization radius is achieved at 2400°K, can now be made. From conservation of energy we find that E_1 the energy liberated is

$$E_1 = C_{al}\, M_{al}\, \Delta T + C_{air}\, M_{air}\, \Delta T + L_{al}\, M_{al} - L_{al_2O_3} M_{al_2O_3} + E_e + E_r$$

where the first two terms result from the specific heat contributions of the aluminum and free air in the fireball, the next two result from the latent heat of fusion of the aluminum and Al_2O_3 (the last latent heat is liberated as the Al_2O_3 fuses and hence is negative) and the last two terms represent the energy lost in expansion of the fireball and in radiation.

The first term is simply

$$C_{al}\, M_{al}\, \Delta T = .27 \text{ cal/gm}^\circ\text{K} \times 1\text{gm} \times 2110^\circ\text{K} = 570 \text{ cal}$$

For the second, we note that the mass of air at 2400°K fills a volume of

$$V_2 = 4/3\, \pi\, R_o^3$$

while from the ideal gas law its original volume was

$$V_1 = V_2\, T_1/T_2 = 4/3\, \pi\, R_o^3\, \frac{290^\circ}{2400^\circ} = 8.54 \times 10^{-3} m^3$$

or .353 moles of air so that, using a molar specific heat we find

$$C_{air}\, M_{air}\, \Delta T = 6 \text{ cal/mole}^\circ\text{K} \times .353 \text{ moles} \times 2110^\circ\text{k} = 4470 \text{ cal.}$$

The third term is just the latent heat of fusion of one gram of aluminum or 94cal and for the fourth we use the latent heat of fusion of Al_2O_3 (244 cal/gm) and the fact that one gram of Al produces 1.88 gm Al_2O_3 so that this term is

$$-L_{al_2O_3}\, M_{al_2O_3} = -244 \text{ cal/gm} \times 1.88 \text{ gm} = -459 \text{ cal}$$

The fifth term is obtained from the previous equation for E_e

$$E_e = 1.26 \times 10^7 [Wt]^{3/4}$$

with $W = 10^{-3}$ Kg and $t = t_o$ the stabilization time = $.0625\ W^{1/3}$ so that

$$E_e = 1575 \text{ cal}$$

Thus using the previous value of E_1 (7400 cal/gm) we find

$$7400 = 570 + 4470 + 94 - 459 + 1575 + E_R$$

or $$E_R \cong 1150 \text{ cal/gm}$$

Considering that this approach has used average values for the temperature (and phase) dependent specific heats and has assumed any processes occurring above 2400^oK are reversed without loss of energy, this value is in very good agreement with the observed value of approximagely 1100 cal/gm.

A.7 Dust Explosion or Fire

The final areas of interest are those of the burning rate temperature and dust flame propagation in aluminum/oxygen mixtures. References 9 and 10 describe a series of experiments on aluminum particle thermodynamics. This discussion will cover three aspects; single particle ignition and burning, particle accretion, and dust ignition both in deflagration and detonation modes.

The ignition temperature of the single aluminum particle depends on the partial pressure of oxygen varying from about 2300^oK at air at 1 atmosphere ($Po_2 = 0.16$) to about 2150^oK at $Po_2 = 1.0$. Ignition temperatures of single carbon, and magnesium particles, vary as 1/r but aluminum does not appear to be r dependent. Due to general heat transfer arguments, ignition times for all particles should vary as r^2. Burning life-times vary as r^2 due to the cenosphere type of burning (diffusion through Al_2O_3 shell) and vary inversely with the oxygen diffusion coefficient. This in turn is linearly proportional to oxygen partial pressure.

Figure A-3 (taken from reference 9) shows data on aluminum particle ignition times. From this data a general equation for the ignition time can be extracted:

$$t_i(\text{sec}) = 2.5 \times 10^{-6} \, (a(\mu))^2 \qquad (U)$$

Burning times in infinite excess oxygen can be estimated from limited data as

$$t_B(\text{sec}) \sim [0.0002 \, a(\mu) - .0004] \qquad (V)$$

Burntime approximately doubles at 50% excess oxygen. Table A-7 gives some data from the literature.

Although not completely verified, the general features of cenospheric particle burning appear to be valid for the case of aluminum in air. Figure A-4 (taken from reference 9) illustrates the features of interest. Diffusion of gaseous aluminum to the combustion zone through the porous alumina shell proceeds until the aluminum is consumed. Figure A-5 (taken from reference 9) plots the ignition and burning conditions as a function of partial pressure.

When a collection of particles (a dust cloud) is considered there are cooperative effects that may take place. The ignition temperature of dust clouds generally varies as $1/\rho$ at least in the range of 1/10 air density. This may be due to several effects: Brownian motion, turbulent density fluctuations, and accretion. The overall tendency would be to produce larger particles and of higher local density which may be easier to ignite.

Particle burning lifetime is extended in a dust cloud. While theory shows that an exact stoichiometric ratio yields an infinite burning time, a stoichiometric ratio of 1.1 (oxygen excess) lengthens burning by nearly 4 times over a single particle case. During burning the oxygen partial pressure is reduced and this effect lengthens the burn.

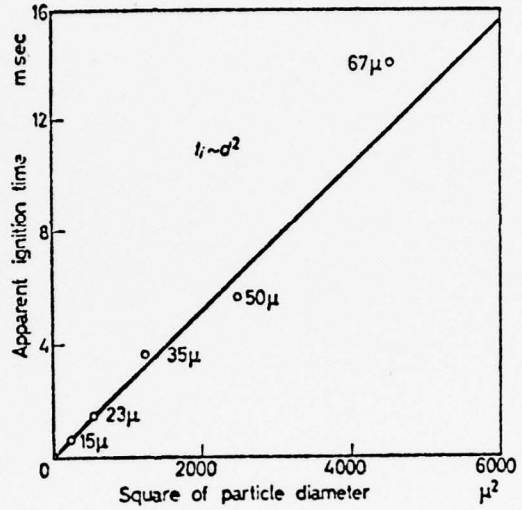

Figure A-3. Experimental apparent ignition time versus particle diameter.

Table A-7

BURNING TIMES IN msec:

DIAMETER μ	EXCESS OXYGEN	
	50%	∞
5	.15	.08
50	7.30	

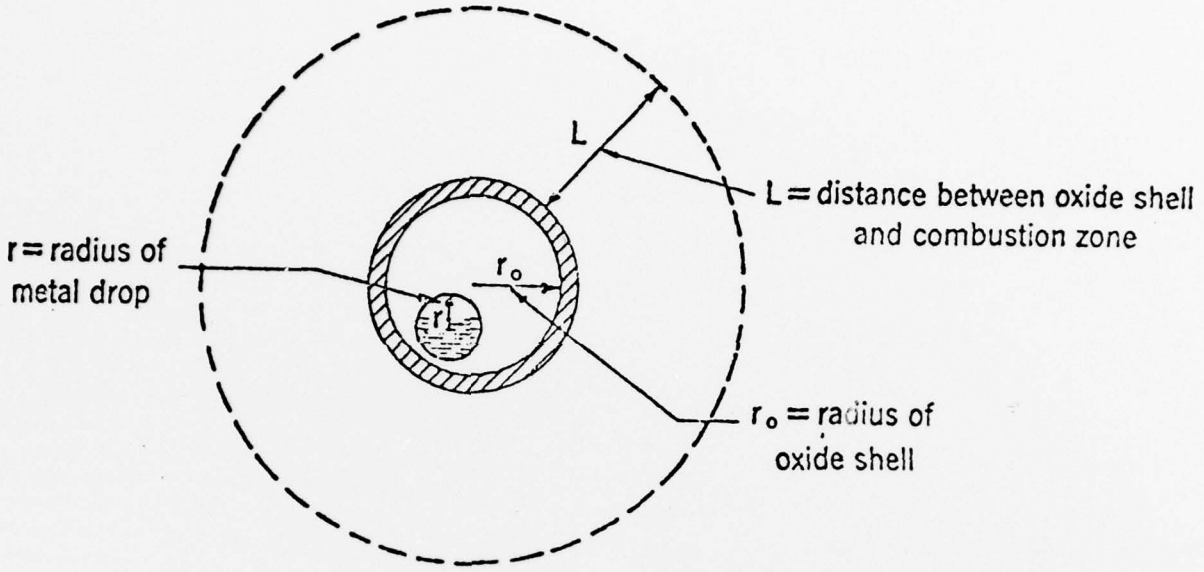

Figure A-4. Cenospheric Particle Burning Model.

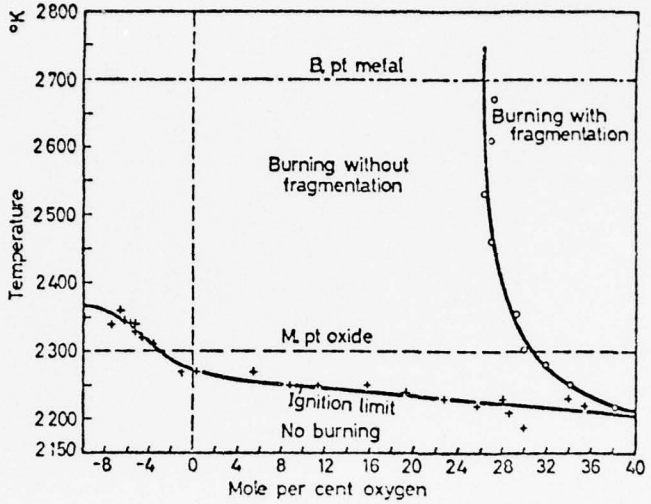

Figure A-5. Experimental Ignition and Fragmentation Limits (35μ diameter Aluminum)

The formulae describing all these phenomenon are complicated but tractable. They will not be repeated here but are given in References 8, 9 and 10.

Dust cloud ignition leads to deflagration (flame) or detonation (shock). In deflagration the burning velocities are of the order of 1 up to 1,000 m/sec, while detonation proceeds at 2000 to 6000 m/sec, and are accompanied by shocks. The various dependencies described are tabulated in Table A-8. Various types of particles may be considered. For example, magnesium burns in about one-half the time of aluminum. Both carbon and magnesium have considerably lower ignition temperatures.

Table A-8. Parametric Variations of Particle Thermodynamic Variables

	Single Particle		Dust Cloud	
	O_2 Partial Pressure P_o	Particle Radius r	Cloud Density δ	Stoic. Ratio s
Ignition Temp. T_i	$P_o^{-\frac{1}{2}}$	$\left[r^{-1}\right]^A$	$\rho - 1$	N/A
Ignition Time t_i	$\left[B\right]$	r^2	N/A	N/A
Burn Time t_b	P_o^{-1}	r^2	N/A	~1ns

A) Verified for carbon and magnesium.

B) Depends on thermal conductivity of gas and T_i.

REFERENCES

1) J. Cockayne, J. Dishon, A. Houghton, T. M. Knasel, "Experimental Studies of Soil Thermal Irradiation - Vol. II." "Thermochemical Pulse Generator Development," DNA 4484F, Science Applications, Inc., April 1977.

2) J. F. Dishon, "Development of a Large Scale Thermal Radiation Simulator," SAI-77-528-SV, 1977, Final report for DNA001-77-C-0200.

3) S. Glasstone, editor, "The Effects of Nuclear Weapons," Superintendent of Documents GOP Washington, D.C. 1964.

4) R. D. Moffat, R. W. Hillendahl, and D. E. Stevenson, "Source and Cloud Transmission Data," SAI/Palo Alto, Report SAI-027-76-PA, October 25, 1976.

5) Letter from T. Sgt. Cummings, USAF to Major J. Mayo, DNA, 23 November 1977.

6) "Pleasanton Experiment," updated report, Sandia Labs informal report.

7) R. W. High, "The Saturn Fireball" in "Prevention of and Protection Against Accidental Explosion of Munitions, Fuels and Other Hazardous Mixture." Annals of the New York Academy of Sciences, Vol. 152, Art. 1, Page 441. October 1968.

8) D. J. Jones, G. C. Goyer and M. N. Plooster, "Shock Wave from a Lightning Discharge," J. of Geophysical Research, 73, p. 3121, May 1968.

9) A. Macek, "Fundamentals of Combustion of Single Aluminum and Beryllium Particles," Hetrogeneous Combustion, p. 204.

10) H. M. Cassel, "Some Fundamental Aspects of Dust Flames," Bureau of Mines Report of Investigation, 6551, 1964.

DISTRIBUTION LIST

DEPARTMENT OF DEFENSE

Assistant to the Secretary of Defense
ATTN: Executive Assistant

Defense Advanced Rsch. Proj. Agency
ATTN: TIO

Defense Documentation Center
12 cy ATTN: DD

Defense Nuclear Agency
ATTN: RAAE, J. Mayo
ATTN: DDST
4 cy ATTN: TITL

Field Command
Defense Nuclear Agency
ATTN: FCPR

Livermore Division Field Command DNA
Department of Defense
ATTN: FCPRL

Under Secy. of Def. for Rsch. & Engrg.
ATTN: Strategic & Space Systems (OS)

DEPARTMENT OF THE ARMY

Atmospheric Sciences Laboratory
U.S. Army Research & Development Command
ATTN: DELAS-EO, F. Niles

BMD Advanced Technology Center
Department of the Army
ATTN: ATC-T, M. Capps
ATTN: ATC-O, W. Davies
ATTN: ATC-O, L. Hayes

Harry Diamond Laboratories
Department of the Army
2 cy ATTN: DELHD-NP

U.S. Army Ballistic Research Labs.
ATTN: Technical Library

U.S. Army Combat Surv. & Target Acq. Lab.
ATTN: C. Markow
ATTN: DELCS-K

U.S. Army Nuclear & Chemical Agency
ATTN: Library

White Sands Missile Range
Department of the Army
ATTN: STEWS-TE-ANL, L. Flores

DEPARTMENT OF THE NAVY

Naval Research Laboratory
ATTN: Code 2627

Naval Surface Weapons Center
ATTN: Code F31
ATTN: C. Infonsino

DEPARTMENT OF THE AIR FORCE

Air Force Geophysics Laboratory
ATTN: OPR, A. Stair
ATTN: OPR, H. Gardner

Air Force Technical Applications Center
ATTN: TFE, J. VonWorkum
ATTN: Technical Library
ATTN: TFR, C. Meneely
ATTN: TFS, M. Schneider

Air Force Weapons Laboratory
ATTN: DE, C. Needham
ATTN: SUL

Space & Missile Systems Organization/SZ
Air Force Systems Command
ATTN: SZJE, H. Hayden
ATTN: SZJ, L. Doan

DEPARTMENT OF ENERGY

Department of Energy
ATTN: Doc. Con. for Classified Library

EG&G, Inc.
ATTN: Doc. Con. for D. Wright

Lawrence Livermore Laboratory
ATTN: Doc. Con. for Technical Information Dept.

Los Alamos Scientific Laboratory
ATTN: Doc. Con. for J. Zinn
ATTN: Doc. Con. for R. Jeffries
ATTN: Doc. Con. for E. Jones
ATTN: Doc. Con. for G. Davis
ATTN: Doc. Con. for Reference Library A. Beyer

Sandia Laboratories
ATTN: Doc. Con. for R. Glasser
ATTN: Doc. Con. for D. Thornbrough

DEPARTMENT OF DEFENSE CONTRACTORS

Aerospace Corp.
ATTN: R. Rawcliffe

General Electric Co.-Tempo
Center for Advanced Studies
ATTN: DASIAC
ATTN: T. Stevens

General Research Corp.
ATTN: J. Ise, Jr.

Information Science, Inc.
ATTN: W. Dudziak

Institute for Defense Analyses
ATTN: H. Wolfhard

Lockheed Missiles and Space Co., Inc.
ATTN: J. Kumer
ATTN: R. Sears

DEPARTMENT OF DEFENSE CONTRACTORS (Continued)

Mission Research Corp.
ATTN: D. Archer
ATTN: D. Sappenfield

Photometrics, Inc.
ATTN: I. Kofsky

R&D Associates
ATTN: F. Gilmore
ATTN: B. Gabbard

R&D Associates
ATTN: H. Mitchell

Science Applications, Inc.
ATTN: D. Hamlin

DEPARTMENT OF DEFENSE CONTRACTORS (Continued)

Science Applications, Inc.
ATTN: J. Dishon

Science Applications, Inc.
ATTN: M. McDonnell
ATTN: M. Knasel
ATTN: J. Cockayne

SRI International
ATTN: W. Chesnut
ATTN: R. Leadabrand

Visidyne, Inc.
ATTN: H. Smith
ATTN: J. Carpenter